ASSESSMENT REPORT
SHEBA PROPERTY – YUKON TERRITORY, CANADA
63°32’8” N, 138°41’29” W, Dawson Mining District

Prepared for:
EUREKA RESOURCES INC.

Prepared by:

AURORA GEOSCIENCES

ASSESSMENT REPORT, 2017 AIRBORNE SURVEY
SHEBA PROPERTY – YUKON TERRITORY, CANADA

SHEBA 1-20, YE32676 – YE32695; SHEBA 21-40, YE32550 – YE32569;
SHEBA 41-60, YE32725 – YE32744; SHEBA 61-69, YE32792 – YE32800;
SHEBA 70-100, YE32501 - YE32531; SHEBA 101-108; YE32745 – YE32752
SHEBA 109-120, YE32402 – YE32413; SHEBA 121-125, YE32696 – YE32700
SHEBA 126-140, YE32435 – YE32449; SHEBA 141-160, YE32570 – YE32589

Dawson Mining District, Yukon Territory, Canada
NTS: 115O10

63°32’8” N, 138°41’29” W
UTM (NAD 83): 614775, 7047320, Zone 7

Work Done from May 6-17, 2017

Effective Date, Nov 16, 2017

Prepared for:
EUREKA RESOURCES INC.
Suite 1100 - 1111 Melville Street
Vancouver, BC. V6E 3V6

Prepared by:
AURORA GEOSCIENCES LTD
34A Laberge Rd.
Whitehorse, Yukon Y1A 5T6

Author:
Carl Schulze, B.Sc., P.Geo., (QP)

TABLE OF CONTENTS

LIST OF FIGURES

LIST OF TABLES

APPENDICES

1. EXECUTIVE SUMMARY

In May of 2017, Eureka Resources Inc. conducted an "Airborne Inductively Induced Polarization" (AIIP) survey combined with an airborne magnetic survey across the Sheba property. The survey was conducted by Geotech Ltd., supervised by Aurora Geosciences Ltd. of Whitehorse, Yukon, and was designed to evaluate for shallow conductive features within the claim block but also to determine the aeromagnetic signature of the property.

In December of 2016, Eureka entered into an agreement to acquire a 100% interest in these properties from two vendors, Panarc Resources Ltd. and Heli Dynamics Ltd. The Sheba property consists of 160 Yukon quartz mining claims covering 3,360 hectares, centered 67 kilometres southeast of Dawson City, Yukon. Although access is currently by helicopter, the northwest corner of the property extends within 1.4 km of a seasonally accessible placer access road extending from the main Black Hills Creek road.

The property is located within the Yukon-Tanana Terrane (YTT), a major accreted terrane comprised of variably metamorphosed, highly deformed intrusive, volcanic and sedimentary rocks mainly Neoproterozoic to late Paleozoic in age, but also includes significant Mesozoic- aged assemblages. The regional stratigraphy, including that of the local area, trends NNW – SSE. The property itself is underlain by two major stratigraphic groups: an aerially extensive assemblage of Permian Sulphur Creek Suite orthogneiss comprised of metamorphosed granodiorite to quartz monzonite; and an extensive package of Proterozoic to Devonian-aged Nasina Series, "Snowcap Assemblage" metaclastic rocks comprised mainly of quartzite, psammite and pelites. The property is located within "Beringia", an area covering west-central Yukon and most of central Alaska and was not affected by Pleistocene glaciation.

The deposit setting is that of "Orogenic Gold", characterized by sizable auriferous quartz veins, potentially up to 1.0 km in length and multiple metres in width. In an orogenic setting there is no evidence of intrusive activity, such as hornfels aureoles or contact metamorphic minerals; hence, "intrusion-related" mineralization is absent. Rather, the structural conduits are district-scale "crustal" faults that allow for hydrothermal fluid movement from a typically deep-seated source. Hard-rock gold mineralization in the Klondike area is considered to be of orogenic origin.

Three main sets of geophysical plots were provided by Geotech Ltd: "Early-Time Gate" and "Mid-Time Gate" plots of the electromagnetic response, and Total Magnetic Intensity (TMI) plots of the magnetic signature. The Early-Time Gate plot reveals the presence of two conductive features crossing at an oblique angle in the west-central property area, indicating shallow structures. The Mid-Time Gate plot revealed conductive features in the northwest and south-central property area. The TMI plot revealed a magnetic "high" feature coincident with the conductive signature in the south-central area, but also delineated a series of NE-SW trending linears in the west-central property area. These linears may represent property-scale structures, potentially amenable to mineralization.

Recommendations for further work include property-wide ridge-and-spur and contour soil geochemical sampling, systematic silt sampling along significant drainages, detailed geological mapping and prospecting. Soil sampling may include traverse lines oriented NW – SE, to test the magnetic linears. A 13-day program, including mobilization and de-mobilization is estimated to cost $88,400.

2. INTRODUCTION

From May 6 to May 17, 2017, Eureka Resources Inc. (Eureka) conducted an "Airborne Inductively Induced Polarization" (AIIP) survey combined with an airborne magnetic survey across the Sheba property. The Sheba property is centered 67 km southeast of Dawson City, Yukon, and is located towards the southern limit of the Klondike placer mining district extending southeast of Dawson City. Aurora Geosciences Ltd. of Whitehorse, Yukon, was retained as primary contractor who retained Geotech Ltd. from Aurora, Ontario, Canada to conduct the airborne survey.

2.1 TERMS OF REFERENCE

The author has been requested to write this report using the following terms of reference:

a) To review and compile all available data obtained by Eureka during its 2017 airborne geophysical surveying program,

b) To provide an Assessment Report to be filed with the Dawson Mining Recorder, Ministry of Energy, Mines and Resources, Government of Yukon.

2.2 TERMS, DEFINITIONS AND UNITS

All costs contained in this report are in Canadian dollars (CDN$). Distances are reported in centimetres (cm), metres (m) and km (kilometres). The term "GPS" refers to "Global Positioning System" with co-ordinates reported in UTM NAD 83 projection, Zone 7. "Minfile Occurrence" refers to documented mineral occurrences on file with the Yukon Minfile, Department of Energy, Mines and Resources, Government of Yukon.

"Mag" and "EM" refer to "Magnetic" and "Electromagnetic" methods respectively of geophysical surveying. "IP" is an abbreviation for Induced Polarization surveying. "AIIP" stands for "Airborne Inductively Induced Polarization" study.

"Ma" refers to million years. "QAQC" refers to "Quality Assurance/ Quality Control".

The term "g/t" stands for grams per metric tonne. The term "ppm" stands for "parts per million, and "ppb" for "parts per billion". ICP-AES stands for "Inductively coupled plasma mass spectroscopy", and AA stands for "atomic absorption".

"CEO" stands for Chief Executive Officer. "NI 43-101" stands for National Instrument 43-101. Elemental abbreviations used in this report are:

Au: Gold
Ag: Silver
As: Arsenic
Pb: Lead
Sb: Antimony
Zn: Zinc

2.3 SOURCES OF INFORMATION

Information on claim tenure, including adjacent properties, and regional geology was provided by the "Yukon Mapmaker Online" website of the Yukon Geology Survey at

http://mapservices.gov.yk.ca/YGS/Load.htm. Information on regional geology was provided by the "Yukon Bedrock Geology" website and by the "YGS Mapmaker Online" website, both available at http://www.geology.gov.yk.ca/Web_map_gallery.html.

3. PROPERTY DESCRIPTION AND LOCATION

3.1 PROPERTY DESCRIPTION

The Sheba property consists of 160 Yukon quartz mining claims covering 3,360 hectares (8,299 acres). The property is centered at 63°32'8" N, 138°41'29" W (UTM NAD 83 coordinates 614775, 7047320, Zone 7) at the confluence of two forks of Wounded Moose Creek east of Eureka Dome. Placer claims in good standing cover the entire extent of both forks of Wounded Moose Creek while a placer lease covers a "right" tributary directly to the northeast. Although no all-season access roads extend on to the property, the stream confluence is located within six kilometres of the main Black Hills Creek access road, and within seven kilometres of the Indian River.

Table 1 shows the claim status of the SHEBA 1-160 block as of Nov 8, 2017.

Table 1: Claim Status, SHEBA claim block

Claim Names	Grant No's	Expiry Date
SHEBA 1	YE32676	10-Jun-21
SHEBA 2	YE32677	10-Jun-22
SHEBA 3	YE32678	10-Jun-21
SHEBA 4	YE32679	10-Jun-22
SHEBA 5	YE32680	10-Jun-21
SHEBA 6	YE32681	10-Jun-22
SHEBA 7	YE32682	10-Jun-21
SHEBA 8	YE32683	10-Jun-22
SHEBA 9-20	YE32684 - YE32695	10-Jun-21
SHEBA 21-30	YE32550 – YE32559	10-Jun-22
SHEBA 31-40	YE32560 - YE32569	10-Jun-21
SHEBA 41-60	YE32725 - YE32744	10-Jun-21
SHEBA 61-69	YE32792 - YE32800	10-Jun-21
SHEBA 70-100	YE32501 - YE32531	10-Jun-21
SHEBA 101-108	YE32745 - YE32752	10-Jun-21
SHEBA 109-120	YE32402 - YE32413	10-Jun-21
SHEBA 121-125	YE32696 - YE32700	10-Jun-21
SHEBA 126-140	YE32435 - YE32449	10-Jun-21
SHEBA 141-160	YE32570 - YE32589	10-Jun-21

There are no current exploration permits for hard rock exploration on the property. Activities allowed under a "Class 1" exploration permit comprise rock, soil and silt geochemical sampling, geological

mapping, trenching (to a limit of 400m^3 per claim), temporary trail construction (to a maximum of 3.0 km) and a maximum of 250 person-days in camp.

A gradation of permits, for Class 2 through Class 4 activities, is required for more significant programs. These programs include diamond drilling and reverse-circulation drilling which have a footprint exceeding Class 1 limits. Larger exploration programs require a "Class 3 Permit", valid for five years and acquired through the local Mining Recorder, Department of Energy, Mines and Resources (EMR), Government of Yukon.

Class 3 permit activities allow for sizable diamond drilling programs (depending on the number of clearings per claim), up to 5,000 m^3 of trenching per claim per year, the establishment of up to 15 km of new roads and 40 km of new trails, and up to 200,000 tonnes of underground excavation work covering the length of the exploration program. A "Yukon Water License" is required if water usage exceeds 300m^3/day. Additional licenses may be required for "Disposal of Special Waste," and a "Consolidated Environmental Act Permit" is required for proper disposal of camp waste and ash resulting from incineration, etc. A "Fuel Spill Contingency Plan" is also required.

All applications for Class 2 through Class 4 require review by the Yukon Environmental and Socioeconomic Board (YESAB). YESAB will provide recommendations on whether the project may proceed, may proceed with modifications, or is not allowed to proceed. Following submission by YESAB, a Decision Body will determine whether to accept the recommendations, and whether a permit will be awarded and, if so, the conditions of the permit.

The property is located within Crown Land in the traditional territory of the Tr'ondek Hwech'in First Nation (THFN).

3.2 Land Tenure and Underlying Agreements

The Sheba property is one of three claim blocks comprising the Luxor project, which also includes the Ophir and Hav properties. In December of 2016, Eureka entered into an agreement to acquire a 100% interest in these properties from two vendors: Panarc Resources Ltd. (50%) and Heli Dynamics Ltd. (50%). The vendors will receive a total of 2,500,000 shares, released as 833,333 shares on the 6, 12 and 18-month anniversaries of the closing date. The vendors also retain a 2% Net Smelter return (NSR) royalty, which Eureka may purchase for CDN$1,000,000.

Figure 1: Sheba Property location map

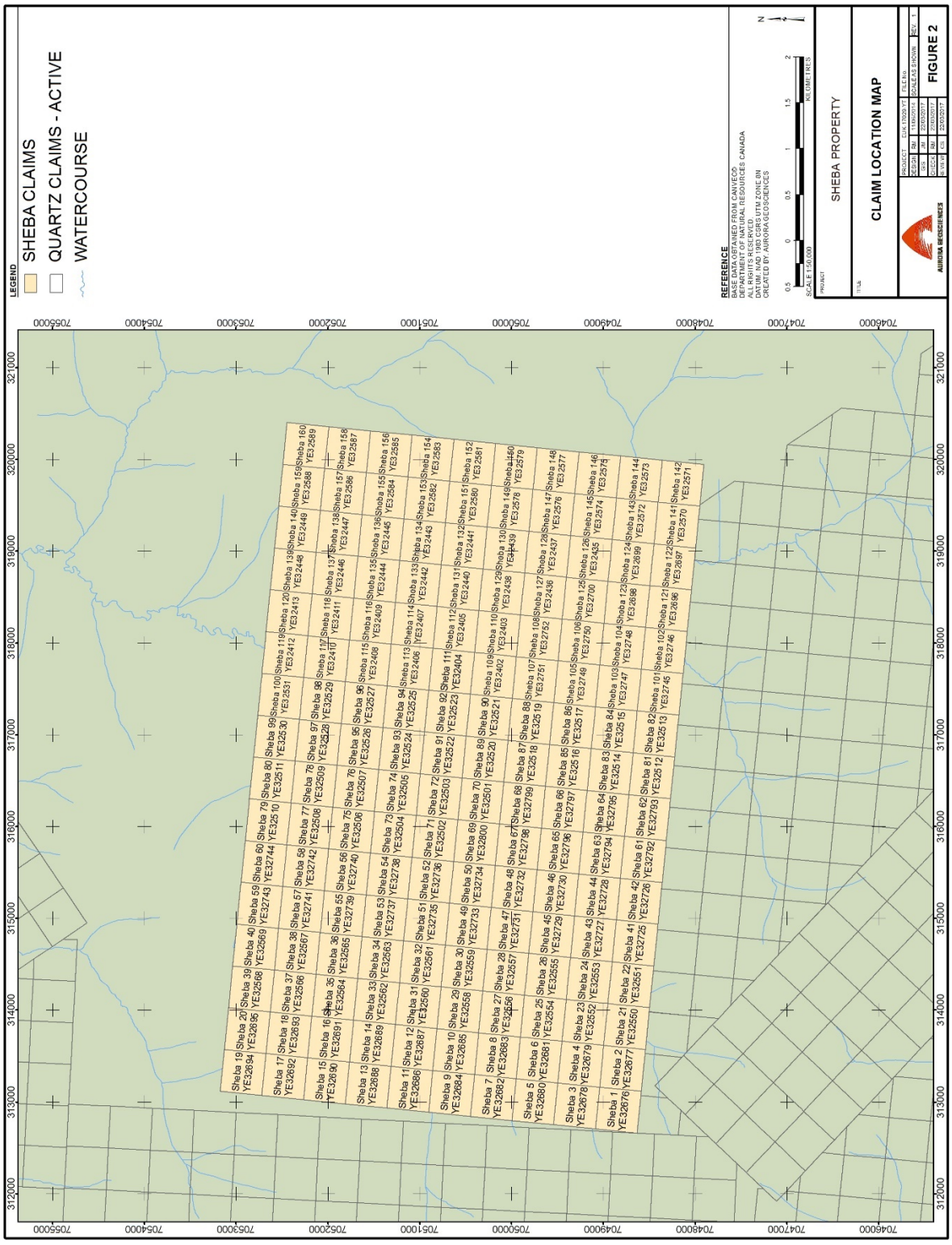

Figure 2: Sheba claim map

4. ACCESSIBILITY, CLIMATE, LOCAL RESOURCES, INFRASTRUCTURE AND PHYSIOGRAPHY

The Sheba property is centered 67 km southeast of Dawson City, Yukon. There is no direct road access; however, the northwest corner is located about 1.4 km from a seasonally serviceable, although retired, placer mine access road. The northern boundary is located 5.9 km south of the main Black Hills Creek placer access road directly south of the Indian River bridge. This road extends southwest from the junction of the Dominion Creek and Sulphur Creek roads, and is seasonally privately maintained by the local operators. The Dominion and Sulphur Creek roads are seasonally maintained by the Department of Highways and Public Works, Government of Yukon, and are accessible from mid-April to mid-October.

Note: Portions of the access roads, including parts of the Black Hills Creek road, may become refurbished and potentially accessible year-round if Goldcorp Inc. commences construction of an access road extending from the North Klondike Highway, near Dawson, to the Coffee Property directly south of the Yukon River.

Access to the property is currently by helicopter from Dawson, with staging sites available along the Black Hills Creek road.

The terrain on the property is moderate, consisting of large rolling hills with few inaccessible areas. Outcrop is scarce and confinedmainly to stream valleys and ridgelines. Elevations range from about 620 metres (2,035 feet) along Wounded Moose Creek at the northern claim boundary to 1,120 metres (3,675 feet) along a ridgeline near the southern boundary. The climate is continental subarctic, with short warm summers having daily highs commonly exceeding 20^{o}C, and long, cold winters with low temperatures averaging -25^{o} to -30^{o}C, although temperatures below -40^{o}C are not uncommon. North facing slopes and some east-facing slopes are typically underlain by permafrost. Precipitation is light to moderate, although showers and thundershowers are common in summer. Maximum snowpack averages from 0.4 to 0.6m, depending on elevation. The field season extends from late May to mid-September, depending on elevation and snow conditions. Drilling may extend into October or November, provided water lines can be kept from freezing.

Dawson City is a full-service community with a population of 1,319 (Wikipedia, 2016). The neighbouring communities in the Klondike area increase the population to roughly 2,000. Dawson City has bulk fuel, grocery and hardware services, abundant accommodation, and government services including the Mining Recorder's office for the Dawson Mining District. Dawson City is located roughly 425 air-kilometres (550 road-kilometres) NNW of Whitehorse along the North Klondike Highway. Whitehorse, Yukon, is a full-service community of about 29,000, with excellent accommodations, groceries, hardware, camp supplies, bulk fuel and expediting services. Whitehorse has a substantial skilled labour force, including professional geoscientists and tradespeople; however, a sizable operation may require staff from outside Yukon.

The property size and moderate terrain are sufficient to accommodate mining facilities, potential mill processing sites, heap leach pads, and waste disposal sites. The moderately rugged topography may require large tailings dams to be constructed for adequate tailings impoundment. There is sufficient water within the property to supply mining and milling operations, including accommodations and drilling. The property is centered about 57 km south of the main electrical transmission line connected to the electrical grid servicing Whitehorse, Mayo, Dawson City and several other Yukon communities.

5. HISTORY

The Sheba property was staked in 2016 by Panarc Resources Ltd. and Heli Dynamics Ltd. The block was optioned to Eureka Resources Inc. in late 2016.

Although the property area was explored for placer gold during the Klondike Gold Rush, no records of activity prior to 2011 within the claim block are known. However, the Wounded Moose Creek confluence is roughly 11 km east of the Eureka Prospect (Yukon Minfile # 115O 057). This prospect and local area underwent several episodes of staking from 1900 through 1920, although little data exists on early exploration. Interest in the prospect resumed in 1988 following the release of RGS stream sediment data, showing an "extremely anomalous" gold value of 89 ppb Au. Several episodes of bedrock mapping, rock, soil and silt geochemical sampling took place from 1988 through 2000. Exploration identified three main mineralized showings: the Allen, Wealth and Childs showings. In 2002, Viceroy Exploration Canada Ltd. conducted mechanical trenching and drilled four reverse-circulation holes; three holes totaling 290 metres on the Allen showing and one 90-metre hole on the Wealth showing (Yukon Minfile, 2017).

Grab samples from the Allen showing, located along the upper reaches of Eureka Creek 1.5 km south of the indicated Minfile location, comprised of milled, clay-rich brecciated quartzite and quartz-muscovite schist returning values to 15 g/t gold. Continuous chip sampling across this zone returned a value of 0.44 g/t gold across 4 metres. At the Wealth showing, located about 3 km south of the Eureka Minfile location, chip sampling returned a value of 0.33 g/t gold across 6.5 metres. Check assaying returned a value of 0.41 g/t gold across the same interval. Reverse-circulation drilling returned a value of 0.66 g/t gold across 8 metres. At the Childs showing, 5 km south of the Minfile location, grab sampling returned values to 3.97 g/t gold with 3.2 g/t silver. All showings are associated with sizable gold anomalies from soil geochemical sampling (Yukon Minfile, 2017).

In 2010, Taku Gold Corp (Taku) acquired the Wounded Moose property from local vendors. The central portion of this property is currently covered by the Sheba claims. In 2011, Taku conducted reconnaissance-style soil geochemical sampling along ridge and spur lines and established two small soil grids in the south-central and northwest areas of the present property. Both grids returned rare anomalous values, to a maximum of 32.4 ppb Au from the north-central grid, and to 113.4 ppb Au from the southern grid (Fekete and Huber, 2011). Background gold values were returned from reconnaissance sampling. Soil sampling also revealed areas of anomalous gold in the northwestern Wounded Moose property area, northwest of the present Sheba block. Gold was analyzed using a 15-gram Aqua Regia digestion, with ICP-MS finish, rather than by fire assay. This area remains held by Taku Gold, although the remainder of the claim block was allowed to lapse.

6. GEOLOGICAL SETTING AND MINERALIZATION

6.1 Regional Geology

The Sheba property is located within the Yukon-Tanana Terrane (YTT), a major accreted terrane comprised of variably metamorphosed, highly deformed intrusive, volcanic and sedimentary rocks (Gordey and Makepeace, 2001). The majority of this terrane ranges from Neoproterozoic to late Paleozoic in age, but also includes significant Mesozoic- aged assemblages. The YTT abuts against Selwyn Basin shelf and off-shelf sedimentary and volcanic rocks to the north, formed along the margins of the Ancient North

American Continent. These two terranes are separated by the 65 Ma Tintina Fault Zone, a major transpressional fault with a dextral displacement of roughly 450 km.

The major stratigraphic orientation in the Sheba area is NNW - SSE, conforming to that of most of southwestern Yukon (Figure 3). Major stratigraphic groups and formations include an aerially extensive assemblage of Permian Sulphur Creek Suite orthogneiss comprised of metamorphosed granodiorite to quartz monzonite (Yukon Geology Survey, "Mapmaker" website). The Sulphur Creek Suite units occur alongside, and may be coeval with, large packages of Permian Klondike Schist, consisting of metaclastic, metavolcanic and minor ultramafic rocks, commonly chloritic, underlying much of the main Klondike placer district. Also prominent in the area is an aerially extensive assemblage of Proterozoic to Devonian-aged Nasina Series, "Snowcap Assemblage" metaclastic rocks comprising mainly of quartzite, psammite and pelites with minor greenstone and amphibolite. Large packages of Mississippian-aged Simpson Range meta-intrusive rocks, consisting of metamorphosed granodiorite, diorite and tonalite, occur to the west of the Snowcap Assemblage package. Late Cretaceous Carmacks Group rhyolitic to rhyodacitic tuffs, welded tuffs and lapilli tuffs occur throughout the project area.

6.2 Property Geology

The Sheba Property is primarily underlain by Permian Sulphur Creek assemblage granite to quartz monzonite intercalated with Proterozoic to Devonian Snowcap Assemblage metasediments (Figure 4). The Sulphur Creek and coeval Klondike Schist assemblages extend northwest-southeast and underlie much of the Klondike area, including parts of the Bonanza, Hunker and Sulphur Creek drainage basins (Yukon Geological Survey, online "Mapmaker"). Regional-scale total magnetic field surveying shows a weak linear magnetic high anomaly extending NNW – SSE, likely indicating the regional trend of stratigraphy.

RGS stream sediment geochemical sampling yielded two anomalous gold values; one of 20 ppb from a site directly east of the property, the other a value of 12 ppb Au from a site in the southwestern property area (Figure 4).

.

6.3 Surficial Geology

The Sheba property is located within "Beringia", an area unaffected by Pleistocene glacial events, extending from west-central Yukon through the majority of central and western Alaska. Surficial deposits consist mainly of colluvium, as well as locales of "loess", consisting of wind-blown fine sand to silt. Bedrock exposure is sparse, due to mechanical and chemical weathering of outcrop, except for areas of very rugged terrain.

Surficial deposits, particularly at lower elevations, have been developed over much longer time periods than post-glacial overburden elsewhere in Yukon. This is particularly applicable to fluvial deposits where local placer gold deposits have developed over much greater time periods than those in glaciated areas.

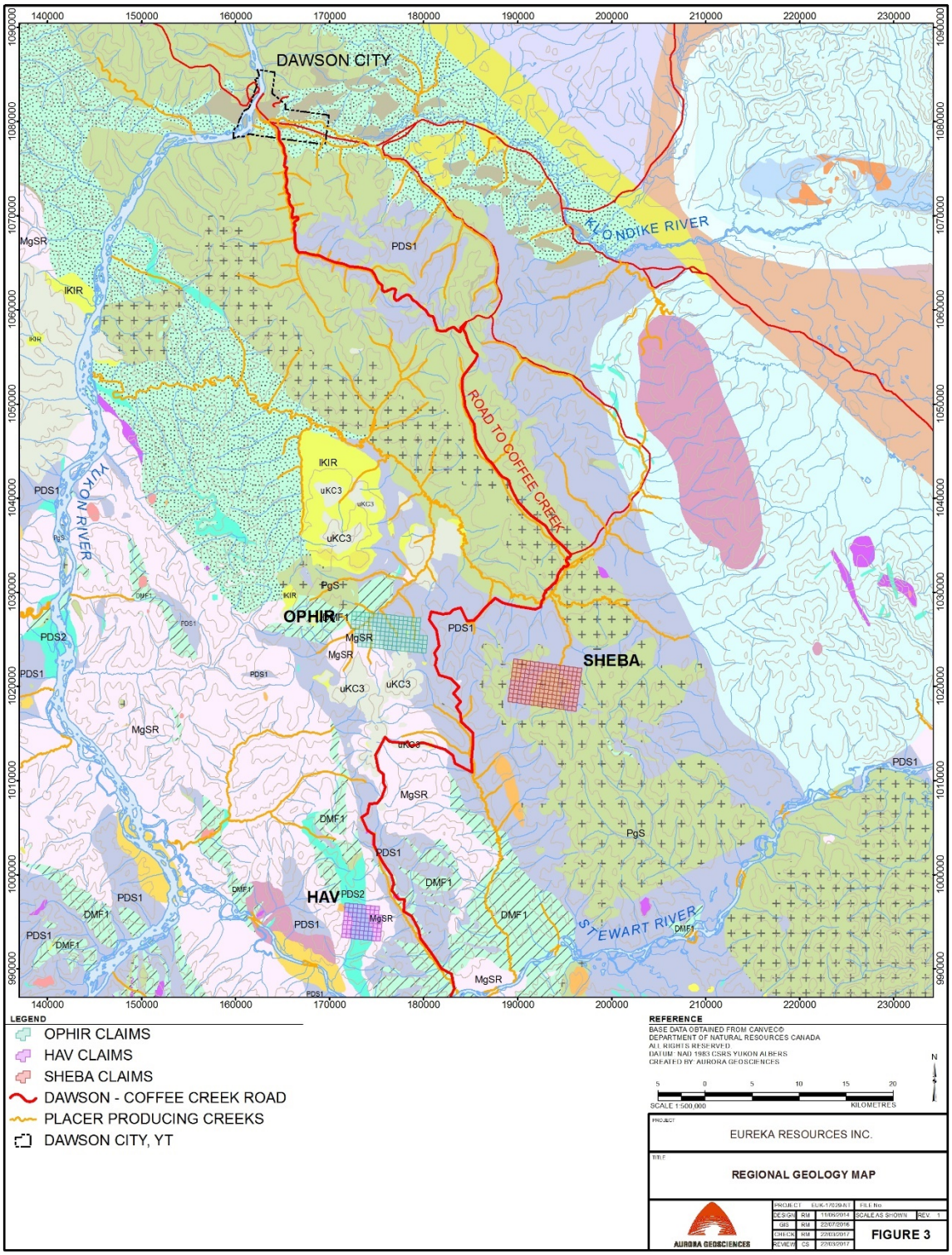

Figure 3: Regional Geology map, Klondike area

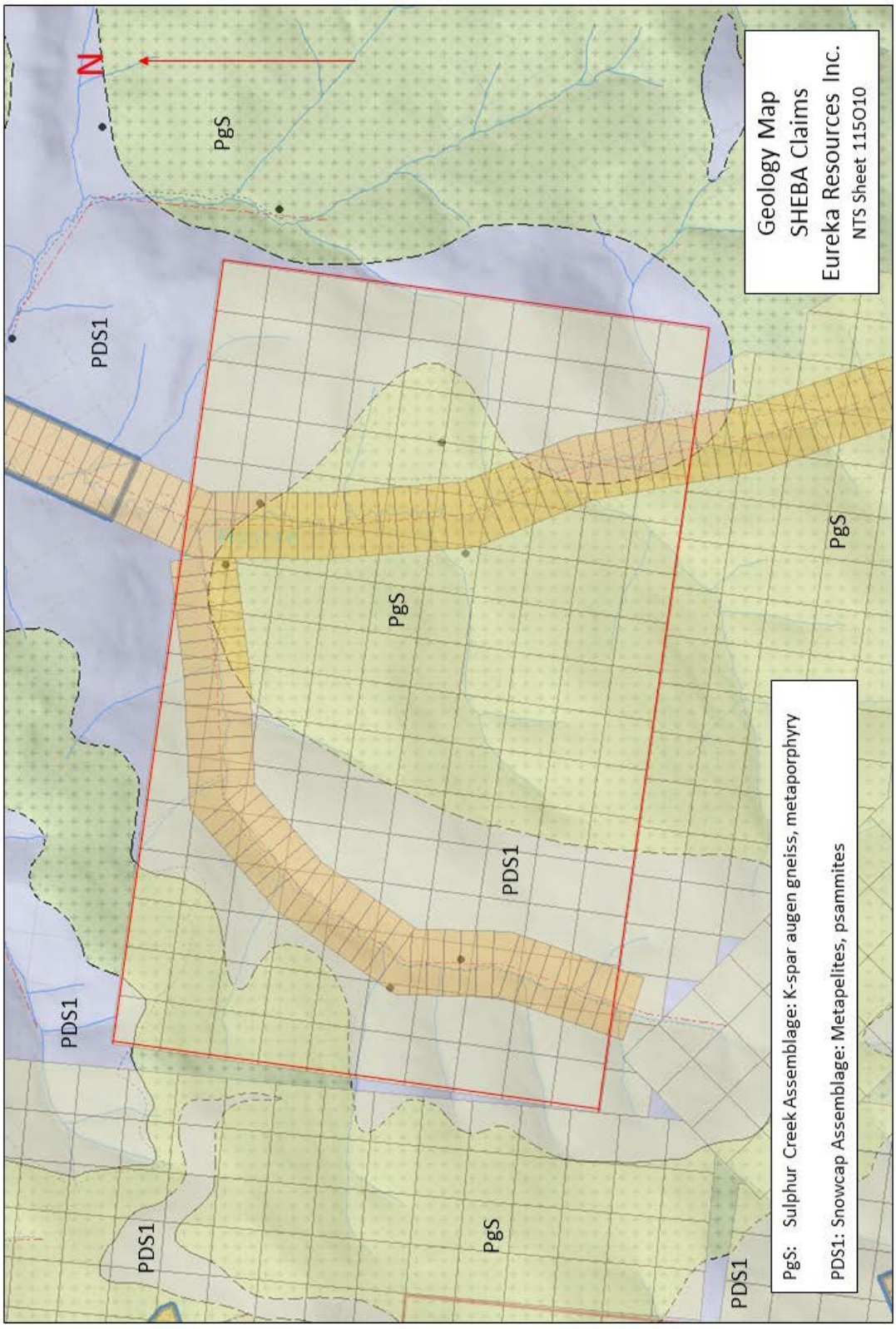

Figure 4: Sheba Property Geology

7.0 DEPOSIT MODELS

The Sheba Property is located towards the southern end of the main Klondike placer mining camp extending southeast from the Klondike River directly east of Dawson. To date, hard rock gold +/- silver occurrences have been ascertained to have an orogenic origin, with fluid movement and emplacement related to deep-seated crustal faults rather than local, shallowly emplaced intrusive bodies. The Klondike area is located within the 70 – 110 Ma Tintina Gold Belt, an arcuate belt of felsic to intermediate intrusions extending from Southwest Alaska through Fairbanks, Dawson City and terminating in the Watson Lake areas. Mineralized zones within the Klondike, to date, do not have the characteristics of intrusion-related systems. Mineralization typically consists of mesothermal quartz veins, hosting gold +/- silver, characterized by the typical pathfinder elements of arsenic (As), antimony (Sb), and, for silver, lead (Pb) and zinc (Zn). The dominant stratigraphic orientation within the Klondike gold camp is NNW – SSE (Figure 3), likely paralleling that of mineralized structures within this district.

The "Orogenic Gold" setting is characterized by larger auriferous quartz veins, potentially to 1.0 km in length and multiple metres in width. Although mineralized quartz veining may be abundant, in the orogenic setting there is no evidence of intrusive activity, such as hornfels aureoles or contact metamorphic minerals, skarn or replacement-style mineralization (Hart and Lewis, 2005). Rather, the structural conduits are district-scale deep-seated "crustal" faults that allow for hydrothermal fluid movement from a typically unknown source. The mechanism for emplacement in local structures is similar to that of intrusion-related veining, whereby mineralized zones develop from fluid movement from along a primary fault conduit and infiltrates into other areas of "structural preparation".

8. EXPLORATION PROGRAM

The 2017 work program consisted of an "Airborne Inductively Induced Polarization (AIIP)" survey combined with an airborne magnetic survey, conducted by Geotech Ltd. from May 6 to 17, 2017. The main geophysical sensors included a "Versatile Time Domain Electromagnetic" (VTEM^{TM} ET) system and a cesium magnetometer (Kwan and Prikhodko, 2017). The flight lines were oriented at an azimuth of N 70^{o} E with a nominal line spacing of 100 metres. Approximately 420 line-kilometres of AIIP and magnetic surveying were flown.

The program was designed to identify resistive units at relatively shallow depths. To achieve this, the AIIP survey consisted of a series of up to 20 readings, or "time gates", spaced a few milliseconds apart, which have been divided into "Early Time Gate" and "Mid Time Gate" plots. The early time gate plot favours identification of shallow, poorly conductive horizons, whereas the mid-time blocks are more adept at identifying deeper, more strongly conductive zones. Plots are provided for each time gate and for "Total Magnetic Intensity" (TMI).

The airborne surveys were supported by two personnel employed by Aurora Geosciences Ltd (Aurora) to place helicopter fuel caches at two locations along the Black Hills Creek Road. The crew also established landing zones for the helicopter and airborne surveying equipment. Following the completion of the field program, all remaining fuel barrels, including empty barrels, and any other materials were removed from the fuel cache sites. The amount of fuel stored per site was less than the threshold for a fuel storage permit.

The barrels were placed by Sean Inkster and this author, Carl Schulze. All fuel drums, full or empty, were removed by Aurora.

Figure 5: Aerial survey by Geotech Ltd.

Figure 6: Aerial survey at landing zone near fuel cache

9. DISCUSSION AND INTERPRETATION

9.1. DISCUSSION

Near-surface sources for AIIP conductors include clays, most metallic sulphides, some oxides, including magnetite, and graphite (Kwan and Prikhodko, 2017). Early time gate plots typically detect surficial deposits, particularly along larger valley bottoms and stream drainages.

The Early-Time Gate plot (Figure 7) displays areas of high conductivity along both forks of Wounded Moose Creek, indicating the presence of surficial clays. However, this plot also indicates the presence of two linear conductors crossing in the west-central property area. Another area of high conductivity occurs in the central property area and is coincident with a ridgeline. Other areas of high conductivity occur in the north-central property area and the northwestern limits of the survey.

The Mid-Time Gate plot (Figure 8) reveals two areas of strong conductivity; one in the northwestern property area, and the other in the east-central area. Both lie along larger watercourses, although the topography in the northwestern anomaly area is fairly rugged, suggesting a non-surficial source. The linear conductors, and the conductor in the central area, are more subdued but still visible. An additional area of interest is a strongly conductive feature, of limited aerial extent, in the south-central property area not visible in the early time gates.

The Total Magnetic Intensity (TMI) plot reveals aerially extensive magnetic “high” signatures in the northern and southeastern property areas (Figure 9), likely representing Proterozoic to Devonian Snowcap Assemblage metapelites and psammites. The TMI plot also reveals a strong magnetic “high” anomaly coincident with the chargeability feature delineated on the Mid-Time Gate plot. Also notable is a NE – SW trending magnetic signature in the west-central area, coincident with chargeability features shown on the Early-Time Gate plot.

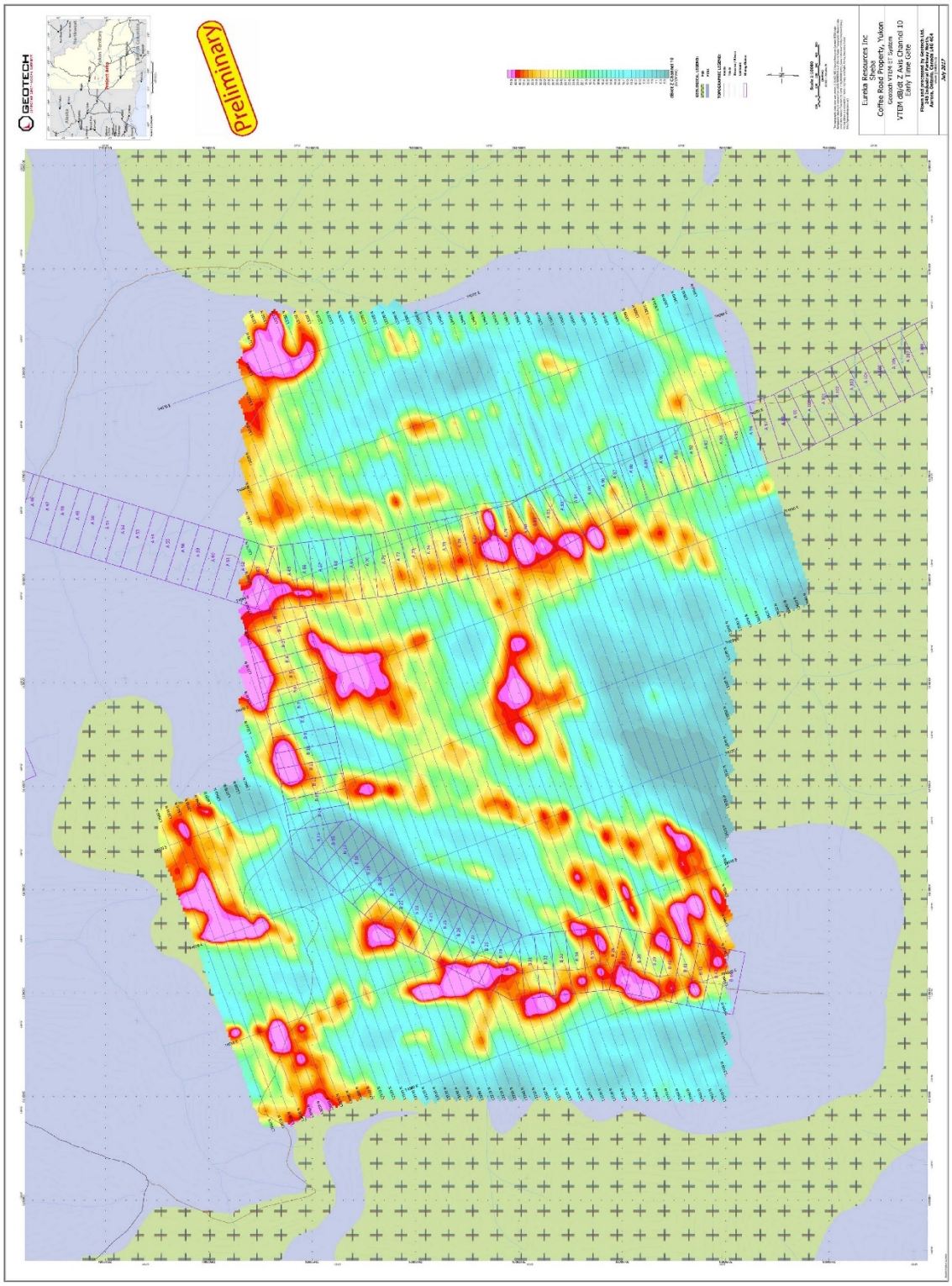

Figure 7: Early-Time Gate EM plot, Sheba property (Geotech Ltd.)

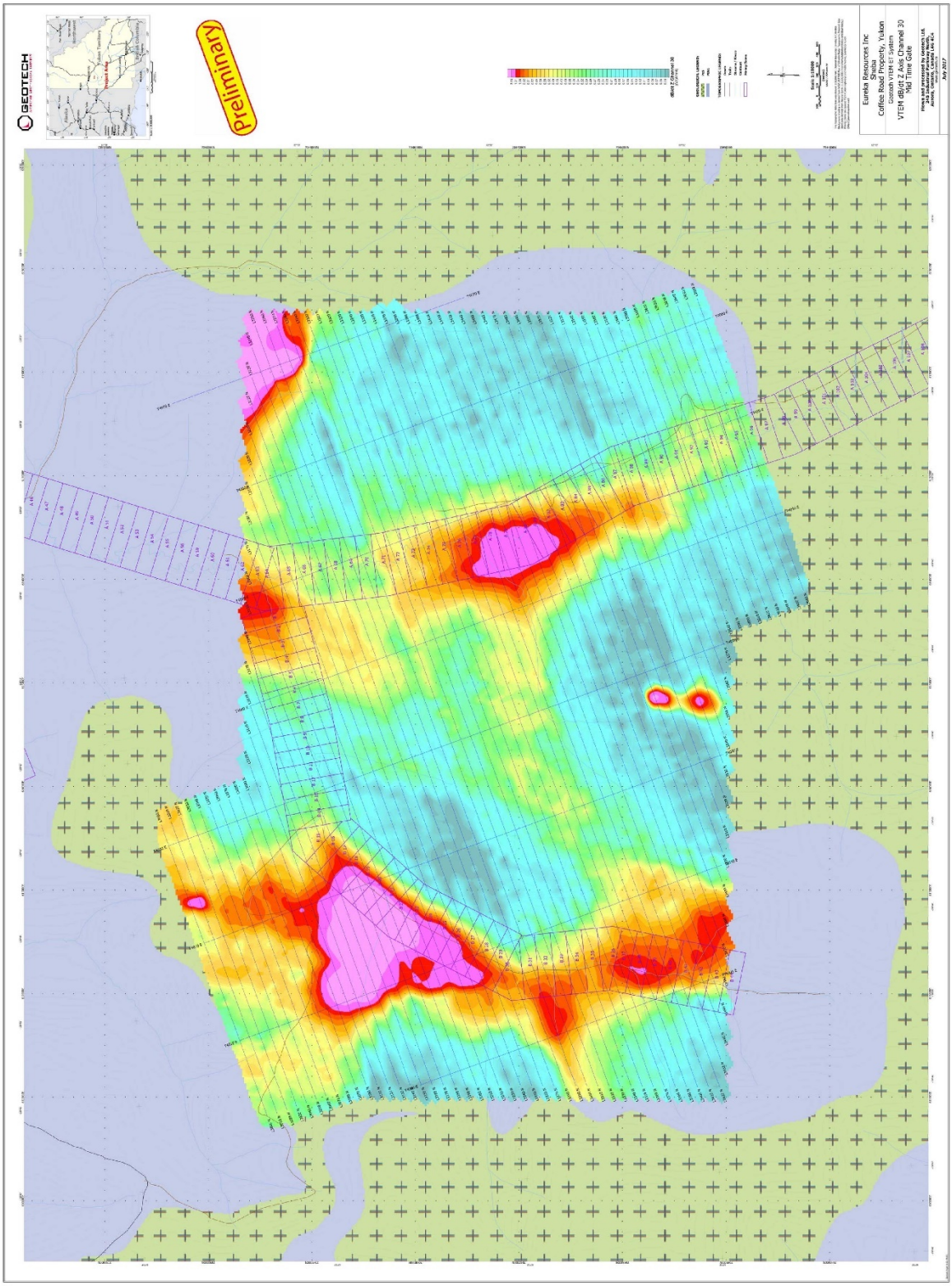

Figure 8: Mid-Time Gate EM plot, Sheba property (Geotech Ltd.)

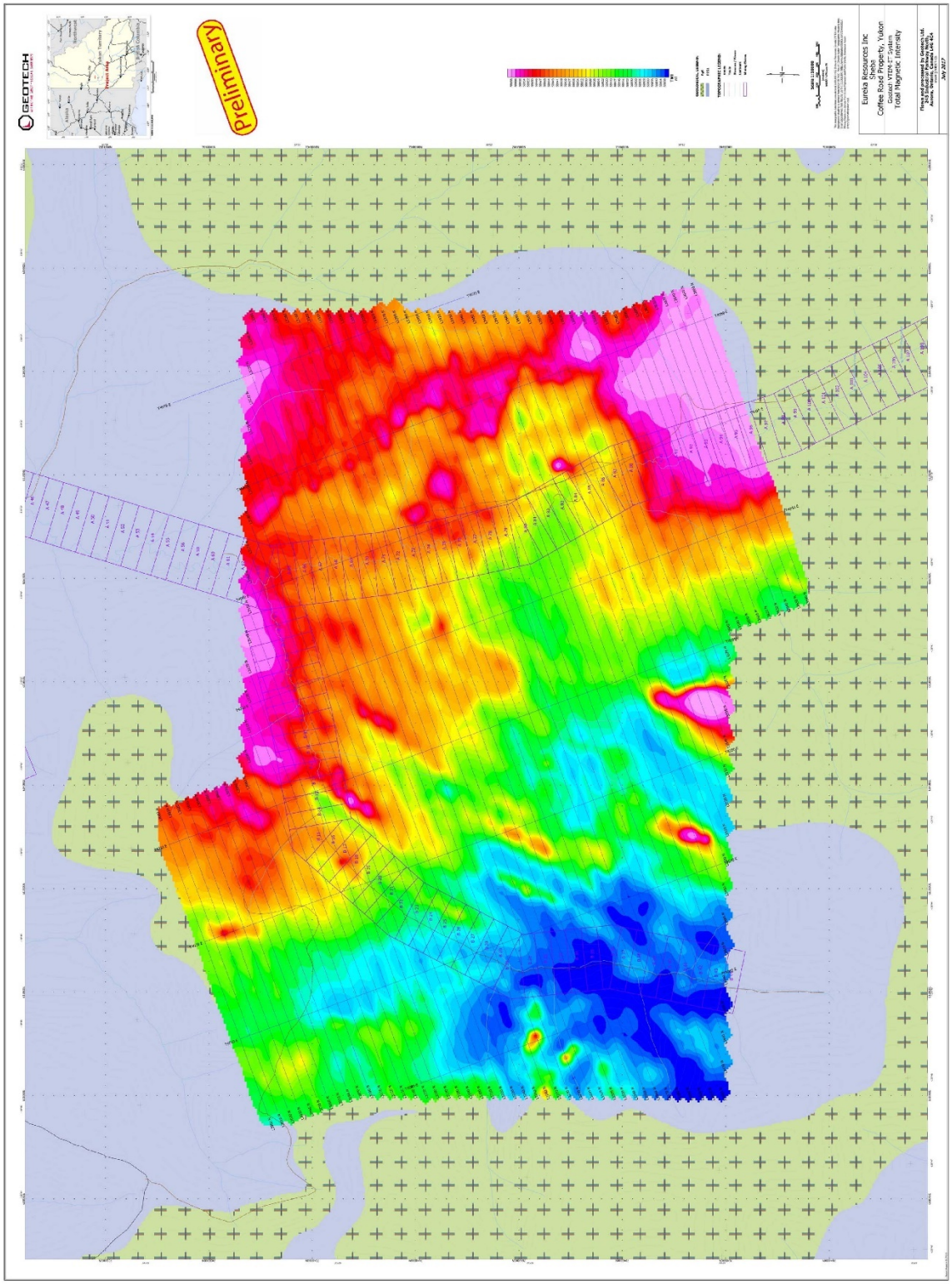

Figure 9: Total Magnetic Intensity (TMI) plot, Sheba property (Geotech Ltd.)

9.2 INTERPRETATION

Review of the Early and Mid-Time gate electromagnetic survey plots, combined with the TMI plot, indicates the presence of a NE-SW trending lineation marked in particular by multiple magnetic high linears and coincident moderately conductive features. The property area has not undergone detailed geological mapping but it is interpreted these features likely represent structural rather than lithological controls. The interpreted structural fabric extends obliquely to the dominant NNW – SSE stratigraphic fabric of west-central Yukon. The lineation is likely to be a fairly local feature, although the full length of the individual linears are unknown and likely extend beyond property boundaries. Property-scale structural features are more likely to be mineralized than district or regional-scale features. Any mineralization in the Sheba property area may be controlled by these features.

One noteworthy feature is an intersection area of two conductive features shown on the Early-Time Gate plot (Figure 10). Intersection areas provide for greater "structural preparation", amenable to movement of metal-bearing hydrothermal fluids, and subsequent emplacement of metal-bearing sulphide mineralization. This may represent a target for subsequent surface exploration.

The magnetic "high" feature on the TMI plot and located in the south-central property area may represent a buried intrusive unit, such as a stock. No Tintina Gold Belt intrusions are known in the area; however, the fairly circular nature of the feature suggests potential for a small stock. The near-absence of a conductive anomaly in the Early-Time Gate plot (Figure 10) versus the Mid-Time plot (Figure 11) suggests the feature is buried.

The majority of the conductive units within both the Early-Time and Mid-Time plots are coincident with the main stream courses, indicating they likely represent surficial deposits. There is a large conductive anomaly in the north-central property area located at a stream confluence (Figure 11). The aerial extent, intensity and fairly rugged local topography, indicate it may not be entirely explained by surficial deposits.

The AIIP report supplied by Geotech includes a plot showing potential gold targets, superimposed on a plot of "Apparent Chargeability" (Figure 13). The west-central property area hosts an intersection of conductive linears (early time gates) with NE-SW magnetic linears. This area is interpreted to be prospective, particularly near the intersection area of the conductive linears seen in the Early-Time Gate plot, within the area of the NE-SW trending magnetic linears.

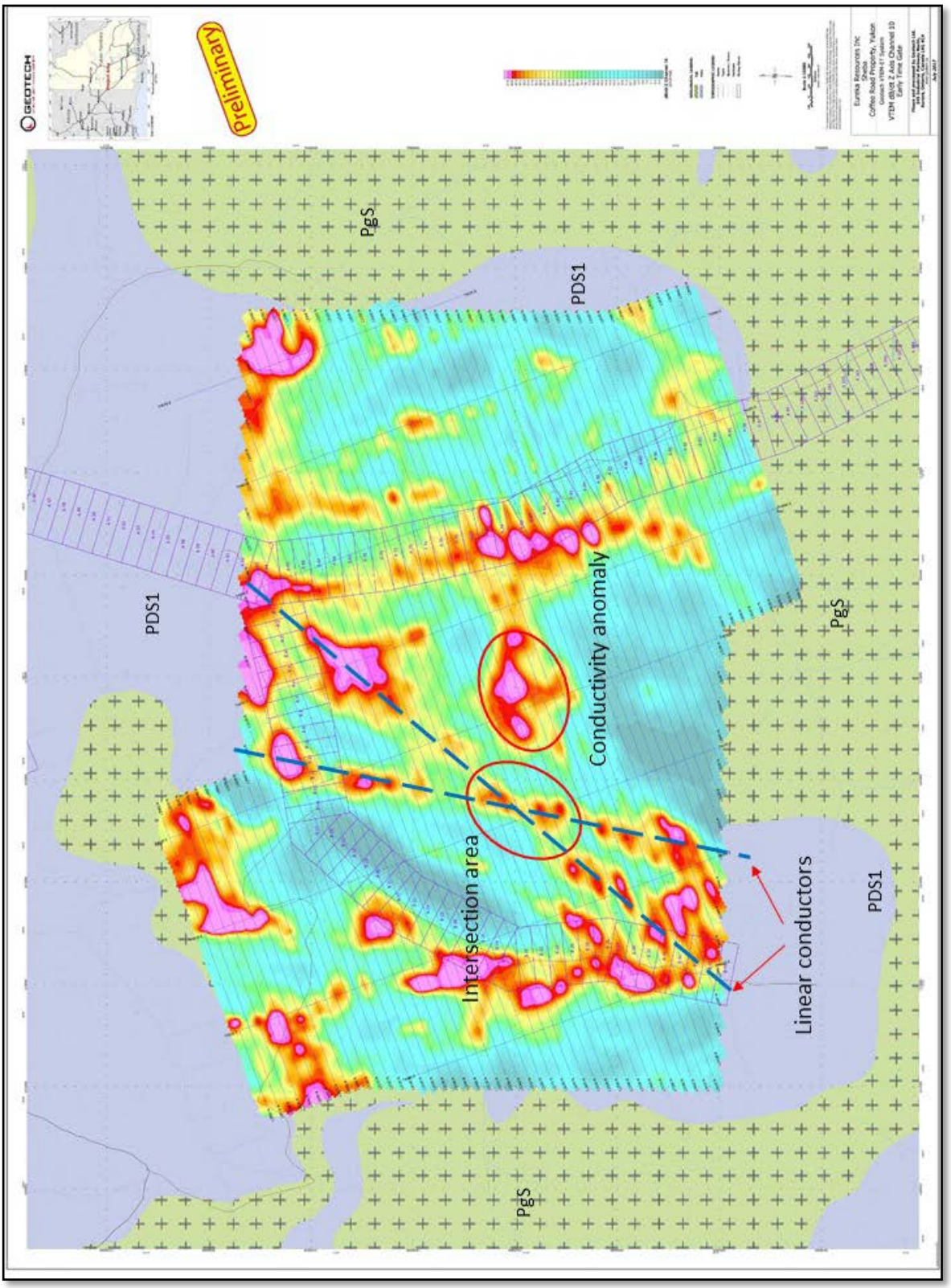

Figure 10: Interpretation of Early-Time Gate EM plot

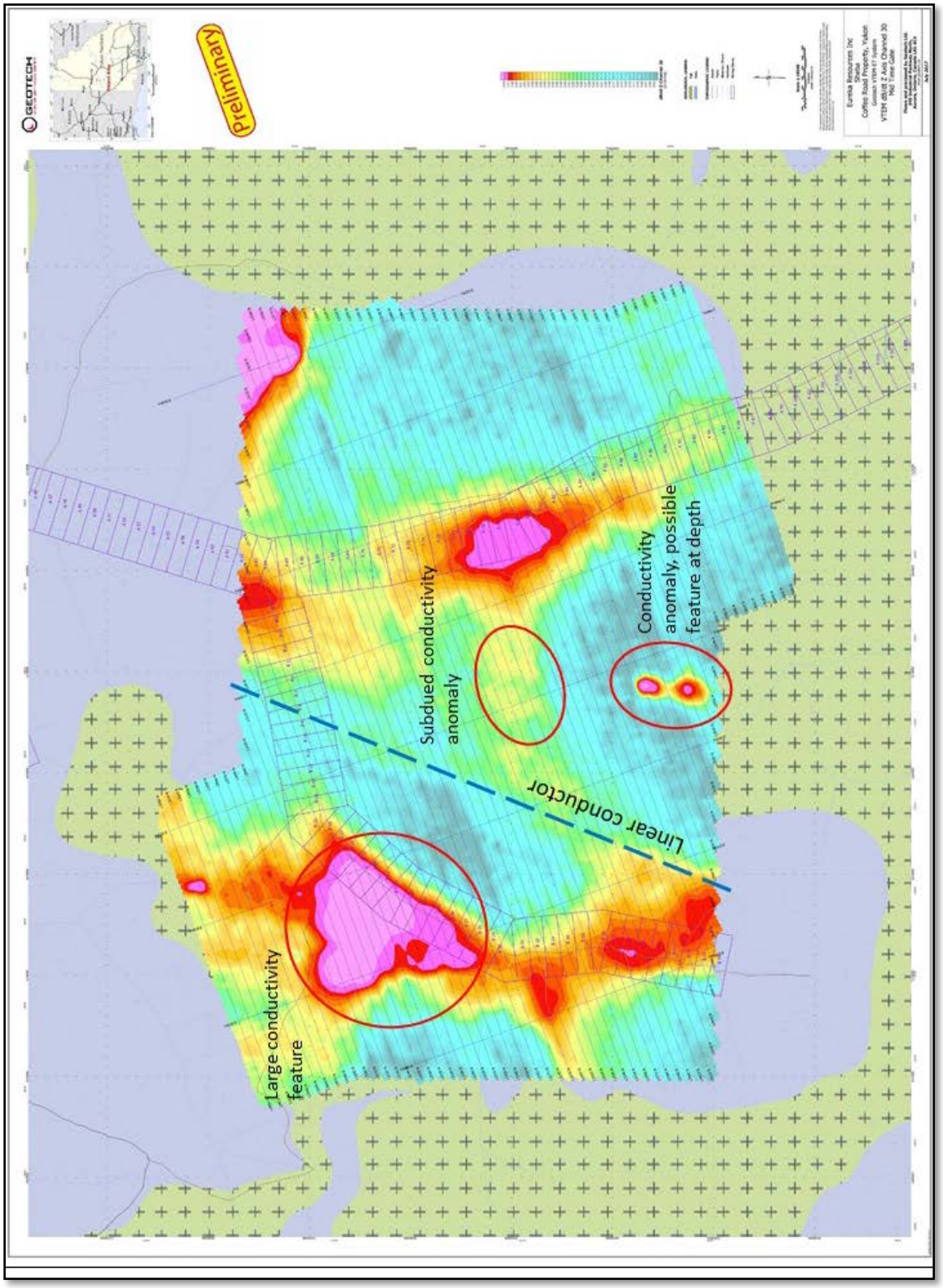

Figure 11: Interpretation of Mid-Time Gate EM plot

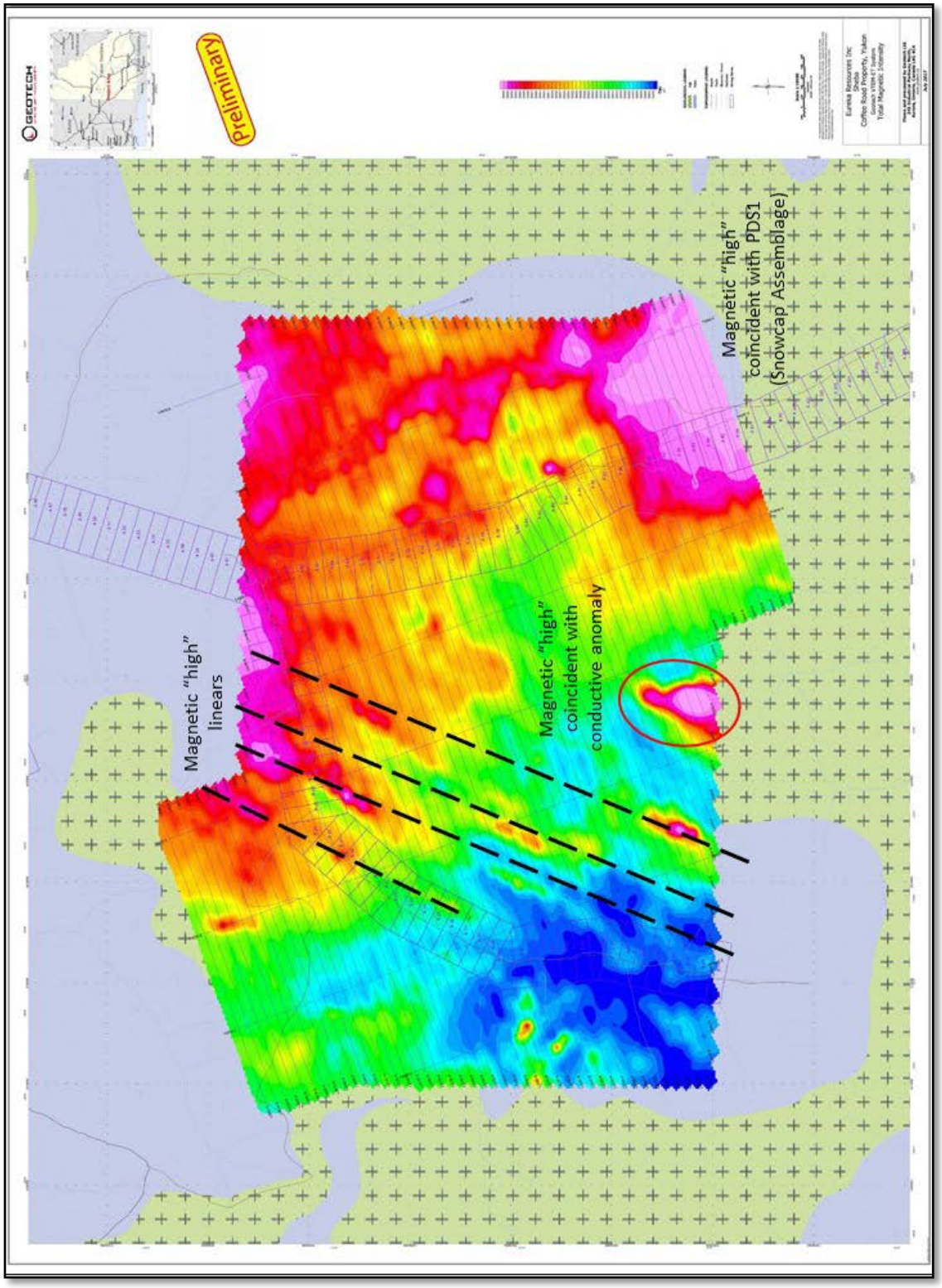

Figure 12: Interpretation of TMI plot

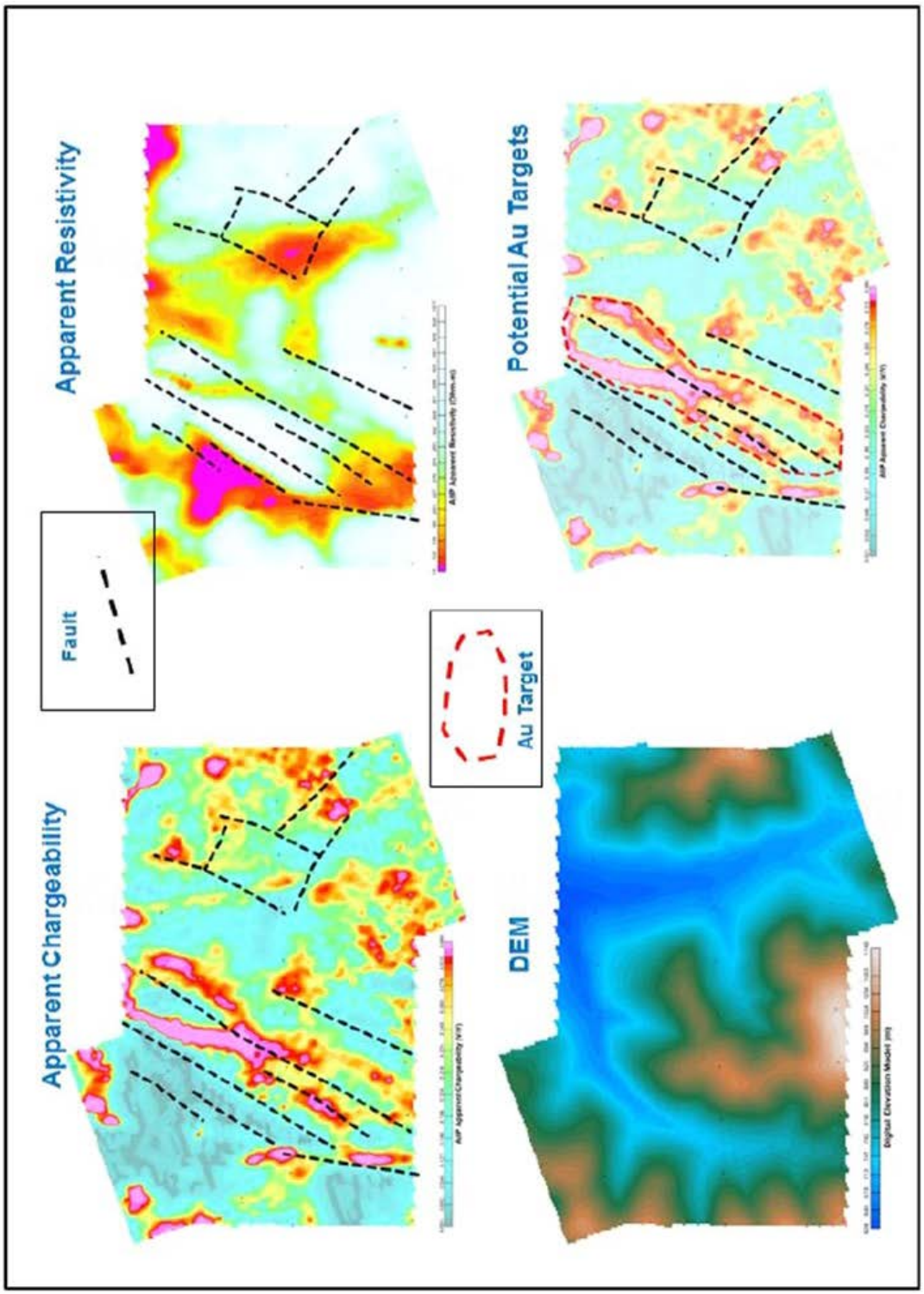

Figure 13: Plots, Interpretation (Kwan and Prikhodko, Geotech Ltd. 2017)

10. CONCLUSIONS

The following conclusions are interpreted from the 2017 AIIP survey on the Sheba property:

- As of November 2017, preliminary electromagnetic Early and Mid-Time gate plots have been provided. The Early-Time Gate plots indicate the presence of at least two conductive linears crossing at a slight angle in the west-central property area. A single, more subdued linear is indicated on the Mid-Time Gate plot, indicating there may be some depth extent to these features.
- Both the Early and Mid-Time Gate plots indicate the presence of a conductive structure in the central property area. This is more likely to be a shallow structure located along an east-west trending ridgeline.
- The Mid-Time Gate plot also shows an aerially extensive conductor in the northwest property area. Although located along a stream confluence, the extent and intensity of this feature, located in an area of significant topographical relief, indicates a partial buried source. Other aerially extensive anomalies suggest near-surface or surficial sources.
- The Total Magnetic intensity (TMI) plot indicates the presence of a NE-SW trending lineation marked by several magnetic linears. These magnetic linears are oblique to the regional trend of stratigraphy, oriented NNW-SSE, and indicate a local property-scale feature. Hydrothermal mineralization tends to be emplaced in smaller structural features such as these, rather than larger, district to regional-scale features.
- The Mid-Time Gate and TMI plots also indicate a sub-rounded anomalous feature, possibly an intrusive body, in the south-central property area. Its near-absence in the Early-Time Gate plot suggests a subsurface source.
- These conclusions are derived from only the early and mid-time gate responses and could change once late-time gate information is delivered.

11 RECOMMENDATIONS

11.1 RECOMMENDATIONS

Recommendations for further work include detailed geological mapping focusing on the magnetic anomaly in the south-central area and the region hosting the magnetic and conductive linears in the west-central area. Mapping should be accompanied by prospecting.

A program of property wide ridge-and spur and contour soil geochemical sampling at a 50-metre station spacing is recommended. Several NW-SE trending traverses, covering the area hosting the magnetic and conductive linears, are suggested. The traverses should be designed to test areas not sampled during the Taku Gold Corp. 2011 program and also provide due diligence sampling of historical anomalous gold samples.

The geochemical sampling program should include stream silt sampling at a 250-metre station spacing along all drainages to locate any anomalous metal content that may escape detection from soil sampling.

This program could be conducted by a four-person crew operating for 13 days, including helicopter-supported mobilization, de-mobilization and travel time from Whitehorse. The program could be staged from Dawson City, with Whitehorse-based expeditor support. Due to the property size, two camp sites would be required in series, with a camp move supplied by helicopter from Dawson City. The program would be completed using eight days of traversing and three days of mobilization from Dawson, including one camp move during the program. Expenditures are estimated at CDN$88,400, including 5% contingency.

Note: Logistical expenses may be reduced if this program is combined with other programs on properties held by Eureka Resources.

11.2 RECOMMENDED BUDGET

Personnel, crew boss: 13 person-days @ $600/day:		$ 7,800
Personnel, 2nd geologist: 13 person-days @ $550/day:		$ 7,150
Personnel, field technicians: 26 person-days @ $450/day:		$11,700
Soil, silt sampling: 450 samples @ $33/sample:		$14,850
Rock sampling: 45 samples @ $39/sample:		$ 1,755
Camp rental (all-in): 13 days @ $130/day:		$ 1,690
Expeditor support (all-in): 4 days @ $1,100/day:		$ 4,400
Helicopter support (Bell 407 or equivalent): 11 hours @ $2,100/hr, incl. fuel:		$ 23,100
Hotel lodging: 4 double rooms @ $135/night:		$ 540
Daily field expenses (including travel): 52 person-days @ $100/day:		$ 5,200
Job prep, camp and equipment:		$ 975
Job prep, Digital data, maps, etc.: 18 hours @ $85/hr:		$ 1,530
Assessment report: 35 hours @ 100/hr:		$ 3,500
	Sub-total:	**$ 84,190**
	5% contingency:	$ 4,210
	Proposed Total:	**$ 88,400**

12. REFERENCES

Fekete, M. and Huber, M, 2011: 2011 Surface Work on the Wounded Moose Property, Dawson Mining District, Yukon. Assessment report #095983, filed with the Dawson Mining Recorder, Ministry of Energy, Mines and Resources, Government of Yukon

Gordey, S.P., Makepeace, A.J. 2001: Bedrock Geology, Yukon Territory, Geological Survey of Canada, Open File 3754; and Exploration and Geology services Division, Yukon Indian and Northern Affairs Canada, Open File 2001-1.

Hart, C.J.R. and Lewis, L.L. 2005: "Gold Mineralization in the upper Hyland River area: a non-magnetic origin". Reference No. YEG2005_08, Yukon Geology Survey.

Kwan, K. and Prikhodko, A. 2017: AIIP Report on a Helicopter-Borne Versatile Time Domain Electromagnetic (VTEM™ ET) and Aeromagnetic Geophysical Survey. Report for Aurora Geosciences Ltd.

Wikipedia, 2017: Population and Weather Statistics for Dawson City, Yukon. Website

Yukon Geology Survey, Energy Mines and Resources, 2017: Website at http://www.geology.gov.yk.ca/

Yukon Mining Recorder, Energy, Mines and Resources, 2017: Website at http://www.yukonminingrecorder.ca/

APPENDIX 1

CERTIFICATE OF QUALIFICATIONS, CONSENT, DATE AND SIGNATURES

I, Carl Schulze, BSc, with business and residence addresses in Whitehorse, Yukon Territory, do hereby certify that:

1. I am a graduate of Lakehead University with a B.Sc. degree in Geology obtained in 1984.

2. I am a Professional Geoscientist registered with the Association of Professional Engineers and Geoscientists of British Columbia (registration number 25393), Association of Professional Geoscientists of Ontario (registration no. 1966) and with the Northwest Territories and Nunavut Association of Professional Engineers and Geoscientists (NAPEG, registration number L3359).

3. I have been employed in mineral exploration as a geologist since 1984, primarily on projects in the Yukon Territory, Northwest Territories, Nunavut, Alaska and British Columbia.

4. I supervised the work described in this report and wrote this report.

5. I have no interest, direct or indirect, nor do I hope to receive any interest, direct or indirect, from Eureka Resources Inc. or any of its properties.

Dated this 16th day of November, 2017 in Whitehorse, Yukon Territory.

Respectfully Submitted,

Carl M. Schulze, BSc. P. Geo.

APPENDIX 2

STATEMENT OF EXPENDITURES

Statement of Expenditures

Invoice #995824, 11-Apr-2017:	$77,689.50
Invoice #995850, 15-May-2017:	$77,491.58
Invoice #995862, 5-June-2017:	$44,135.47
Invoice #995902, 1-Jul-2017:	$27,860.47
	Total: $222,177.02

Pro-rated: 34.5% of total flight lines: $76,649.35

APPENDIX 3

GEOTECH LTD. REPORT

VTEM™ ET

AIIP REPORT ON A HELICOPTER-BORNE VERSATILE TIME DOMAIN ELECTROMAGNETIC (VTEM™ ET) AND AEROMAGNETIC GEOPHYSICAL SURVEY

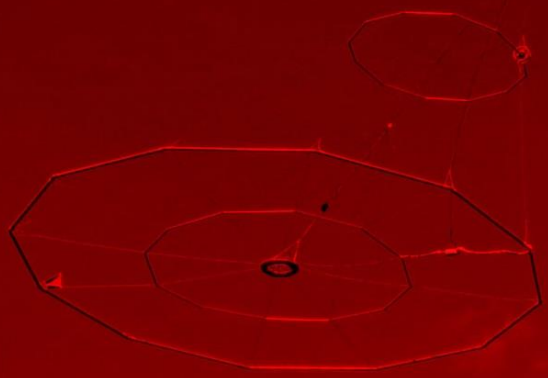

PROJECT:	OPHIR, SHEBA, HAV, TAK, AND ETTA
LOCATION:	COFFEE ROAD PROPERTY, YUKON
FOR:	EUREKA RESOURCES INC.
SURVEY FLOWN:	MAY 2017
PROJECT:	GL170103

Geotech Ltd.
245 Industrial Parkway North
Aurora, ON Canada L4G 4C4

Tel: +1 905 841 5004
Web: www.geotech.ca
Email: info@geotech.ca

GEOTECH
AIRBORNE GEOPHYSICAL SURVEYS

TABLE OF CONTENTS

LIST OF FIGURES

LIST OF TABLES

APPENDICES

EXECUTIVE SUMMARY

AIIP report on VTEM™ ET surveys, Coffee Road Property, Yukon

During May 6th – 17th 2017 Geotech Ltd. carried out a helicopter-borne geophysical survey over the A1-Ophir, A2-Sheba, A3-Hav, A4-Tak, and A5-Etta blocks situated within the Coffee Road Property, Yukon.

Principal geophysical sensors included a versatile time domain electromagnetic (VTEM™ ET) system, and a caesium magnetometer. Ancillary equipment included a GPS navigation system and a radar altimeter. A total of 1218 line-kilometers of geophysical data were acquired during the survey.

Geotech Ltd carried out airborne inductively induced polarization (AIIP) chargeability mapping of the VTEM data.

Final AIIP products are:

- AIIP databases;
- AIIP apparent chargeability and resistivity grids;
- AIIP report.

1. SURVEY LOCATION

The VTEM survey blocks were located south of Dawson City, Yukon, Figure 1.

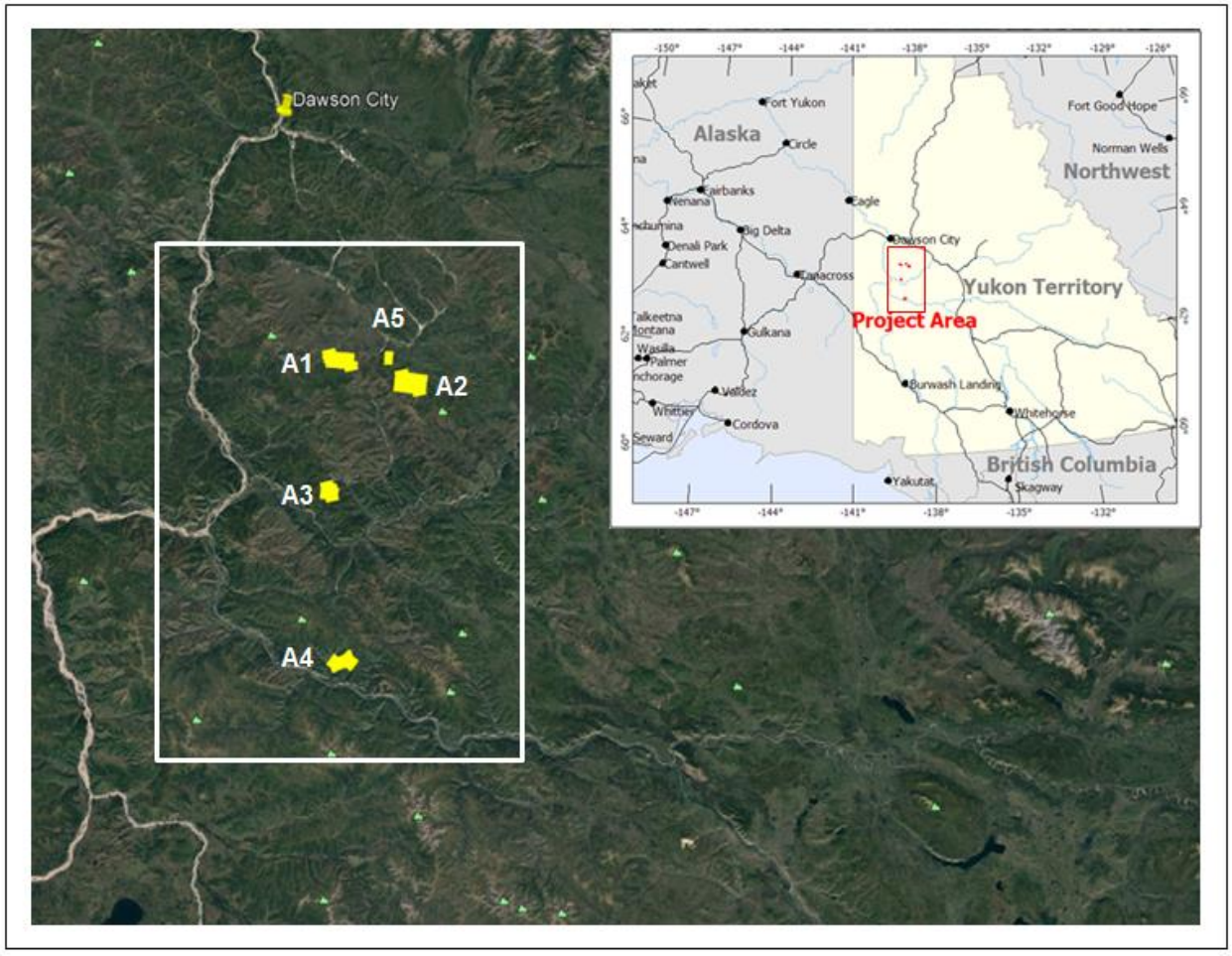

Figure 1: VTEM survey location (image from Google Earth).

The survey areas were flown in an east to west (N 70° E azimuth) direction over A1 (Ophir), A2 (Sheba), and A3 (Hav) blocks. The A4 (Tak) block was flown in a northeast to southwest (N 30° E azimuth), and the A5 (Etta) block was flown in a north to south (N 178° E azimuth). The nominal traverse line spacing is 100 metres.

Blocks A1, A5 and A2 are located approximately 60 kilometers SSE of Dawson City, Yukon. A4 is located approximately 126 kilometers south of Dawson City.

2. AIRBORNE INDUCTIVELY INDUCED POLARIZATION (AIIP)

The objective of AIIP mapping of VTEM data from is to derive Cole-Cole apparent chargeability and resistivity maps for a fixed frequency factor c.

2.1 AIIP EFFECTS IN VTEM DATA

Airborne VTEM™plus data from Coffee Road Property reflect mainly two physical phenomena in the earth:

1. Electromagnetic (EM) induction, related to sub-surface conductivity and governed by Faraday's Law of induction;

2. Induced polarization (IP) effect, related to the relaxation of polarized charges in the ground (Pelton et al., 1978, Weidelt, 1982, Kratzer and Macnae, 2012 and Kwan *et al*., 2015a and 2015b);

For mineral exploration, near-surface sources of AIIP are clays through membrane polarization (electrical energy stored at boundary layer) and most metallic sulphides, some oxides (i.e. magnetite) and graphite through electrode polarization (electrical charges accumulated through electrochemical diffusion at ionic-electronic conduction interfaces).

The absence of negative transients does not preclude the presence of AIIP (Kratzer and Macnae, 2012). The case is clearly illustrated in Figure 2, showing forward modeled VTEM decays over a chargeable half-space of different chargeabilities, using the Cole-Cole relaxation model (Appendix A). As chargeability value increases from m=0 (purely inductive), the rate of VTEM decay increases (pulling down) also in mid-times and eventually crosses into the negative when m≈0.8 V/V. But for vast majority of m values less than 0.8 V/V, there are no negatives in the VTEM decays.

The amount of deviation from the ideal inductive response of a half space with resistivity ρ_0 is a measure of the strength of AIIP.

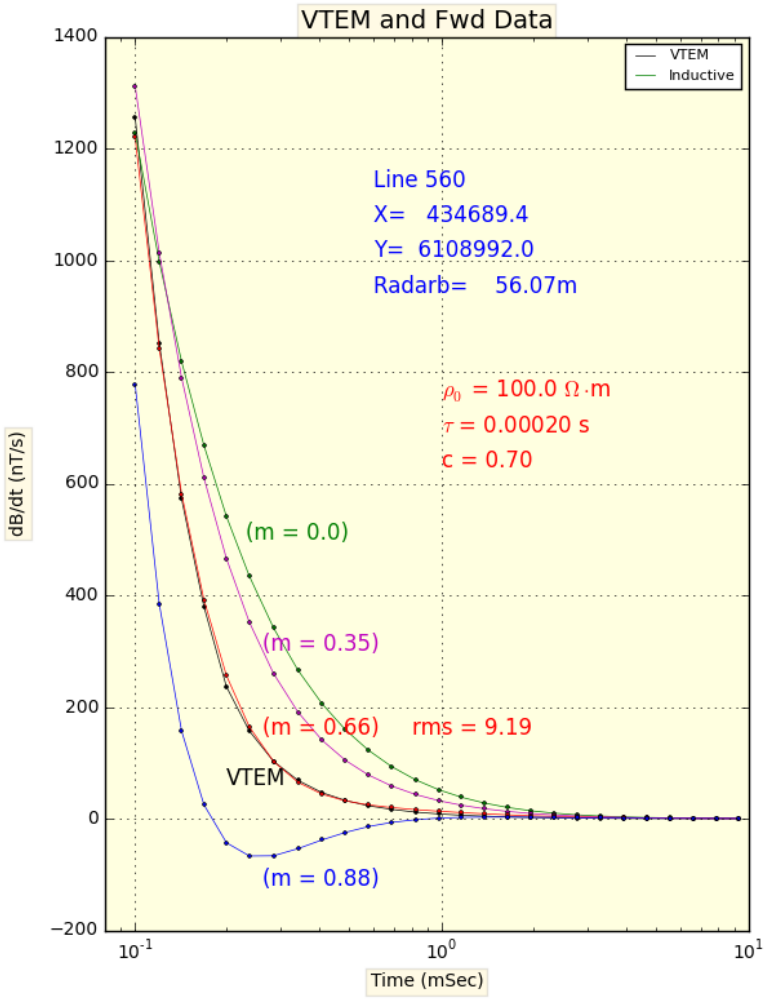

Figure 2: Forward modelled VTEM decays for different chargeability m values; the observed VTEM decay (black) was from Mount Milligan, British Columbia, fits well with the modeled decay (red) with m=0.66.

Numerous negative transients are observed in the VTEM data from A3 and A4. Some of them from L7120 of A4 (Tak) block are shown in Figure 3, providing unequivocal pieces of evidence that there are AIIP effects in the VTEM data.

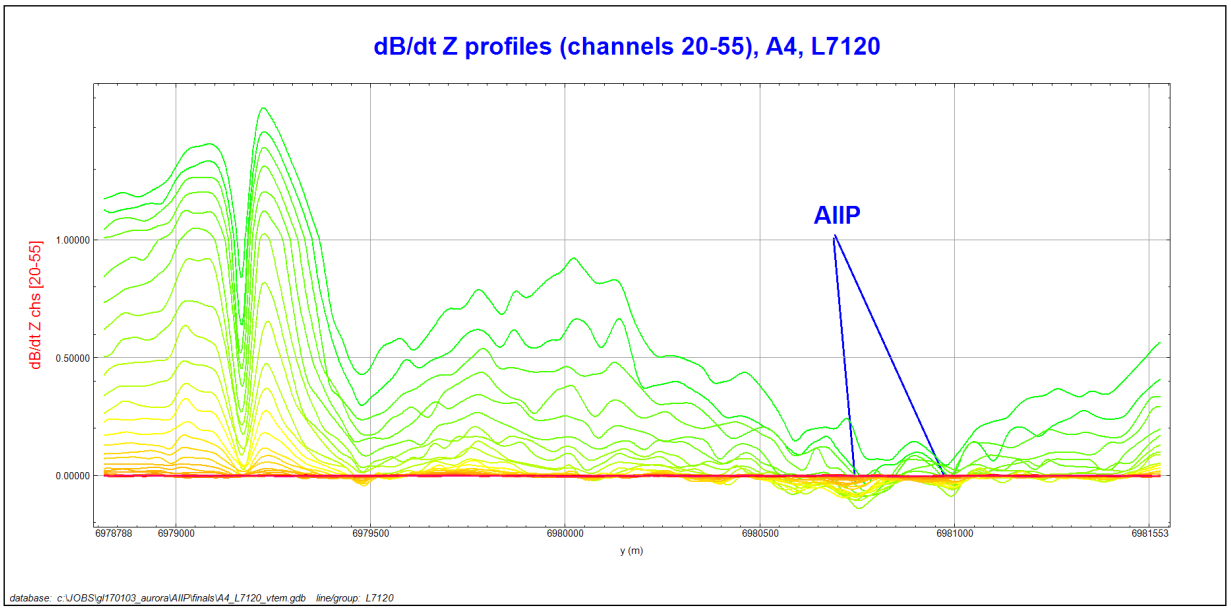

Figure 3: AIIP anomalies in L7120, A4 (Tak) block.

2.2 AIIP MAPPING

VTEM decays associated with AIIP can be studied using the empirical Cole-Cole complex resistivity model (Cole and Cole, 1941 and Pelton *et al*., 1978), shown in equation (1).

$$\rho(\omega) = \rho_0 \left[1 - m\left(1 - \frac{1}{1 + (i\omega\tau)^c}\right)\right] \qquad (1)$$

In the equation above, ρ_0 is the DC resistivity, m ($0 \leq m \leq 1.0$) is the chargeability in (V/V), τ is the Cole-Cole time constant in second, $\omega = 2\pi f$, and c ($0 \leq c \leq 1.0$) is the frequency factor. The four parameters (ρ_0, m, τ and c) are characteristic of a polarizable ground.

In general, chargeability m and Cole-Cole time constant τ depend on the quantity and size of polarizable elements in the ground (Pelton *et al*., 1978). The frequency factor describes the size distribution of the polarizable elements (Luo and Zhang, 1998). When c=1, the time-domain decay modelled by Cole-Cole model represents the Debye decay, and when c=0.5, the time-domain decay is the Warburg decay (Wong, 1979).

The extraction of the four Cole-Cole parameters (ρ_0, m, τ and c) from airborne VTEM data is a difficult task. Kwan *et al*. 2015a developed an algorithm, based on Airbeo from CSIRO/AMIRA[1] (Chen & Raiche 1998; Raiche 1998), to extract the (ρ_0, m and τ) parameters while the frequency factor is fixed. There are two deficiencies in the algorithm; one, the precision of the derived (m_o, τ_o) depends on the final mesh size, and two, many of the inversions at the mesh locations far away from (m_o, τ_o) are not necessary.

[1] Commonwealth Scientific and Industrial Research Organization and Amira International;

An improved version of the AIIP mapping algorithm has since been developed by Geotech (Appendix A). The new method applies the Nelder-Mead Simplex minimization (Nelder and Mead, 1965) in the two-dimensional (m,τ) plane. At each required test point (m_i, τ_i), the optimal background resistivity $\rho_0$is found by one-dimensional Golden-Section minimization for the user specified resistivity range. The algorithm uses only Airbeo's forward modeling kernel, which can generate synthetic VTEM data with high precision. The Nelder-Mead (NM) search algorithm is more efficient than the grid search method by Kwan *et al*. 2015a, and generates much more precise apparent chargeabilities, resistivities, and IP relaxation time constants. The improved NM AIIP mapping algorithm has been used to process the airborne time-domain electromagnetic data from numerous VTEM surveys since 2015.

AIIP processing is applied to VTEM data desampled to 10 m interval.

2.3 DETERMINATION OF FREQUENCY FACTOR C

The Geotech AIIP chargeability mapping algorithm described in Appendix A requires fixed frequency factor c, while the DC resistivity, chargeability m and IP relaxation time constant τ are allowed to vary. The determination of frequency factor c for selected VTEM data is carried out by interactive forward modelling software, also based on Airbeo from CSIRO/AMIRA. The locations of selected VTEM decays for c calculations, over EM induction time-constant TAU, are shown in Figure 4. Eighteen (18) frequency factor c values are determined from the selected VTEM decays. All c values equal to 0.7.

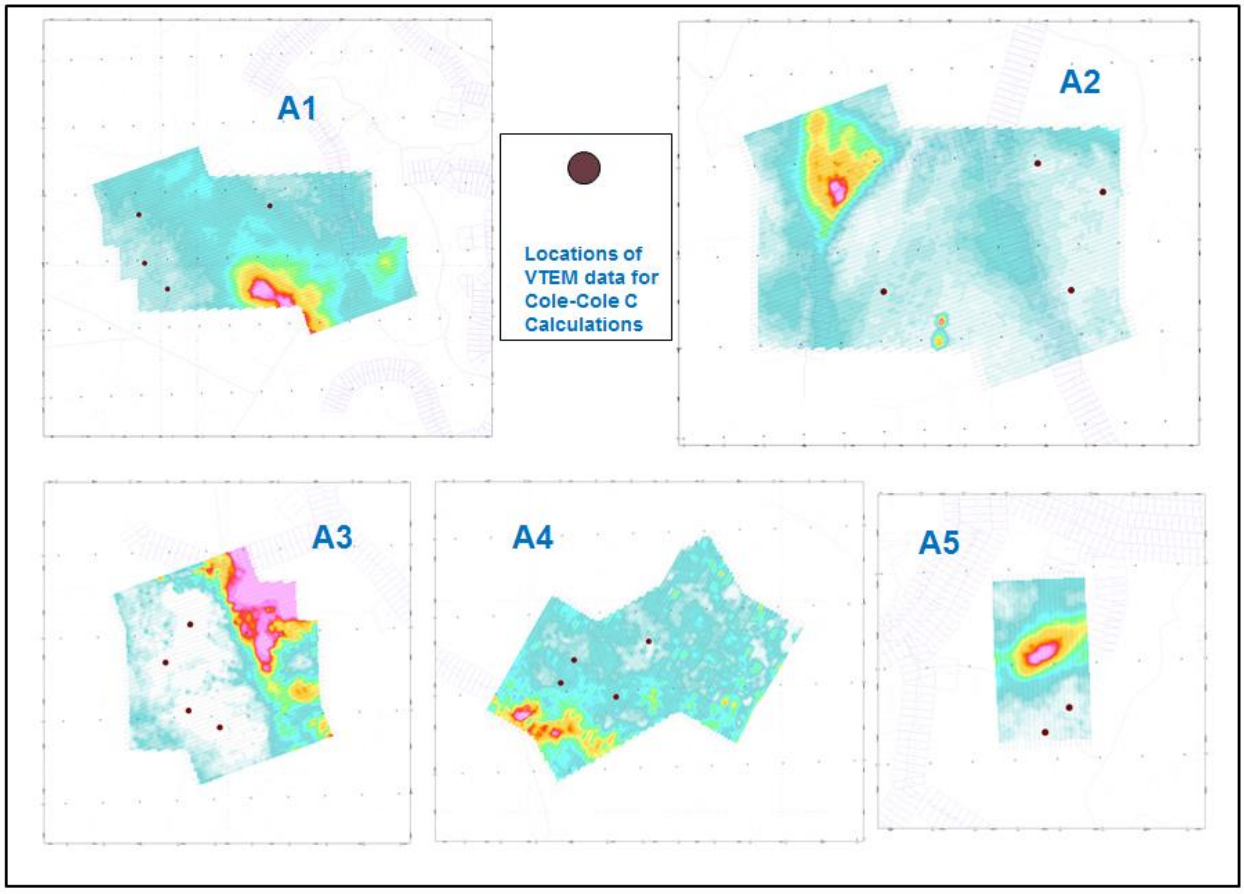

Figure 4: The locations of VTEM decays used for frequency factor c determination over time-constant TAU, areas A1 to A5.

Full Cole-Cole forward modelling results for four selected VTEM decays are shown in Figure 5.

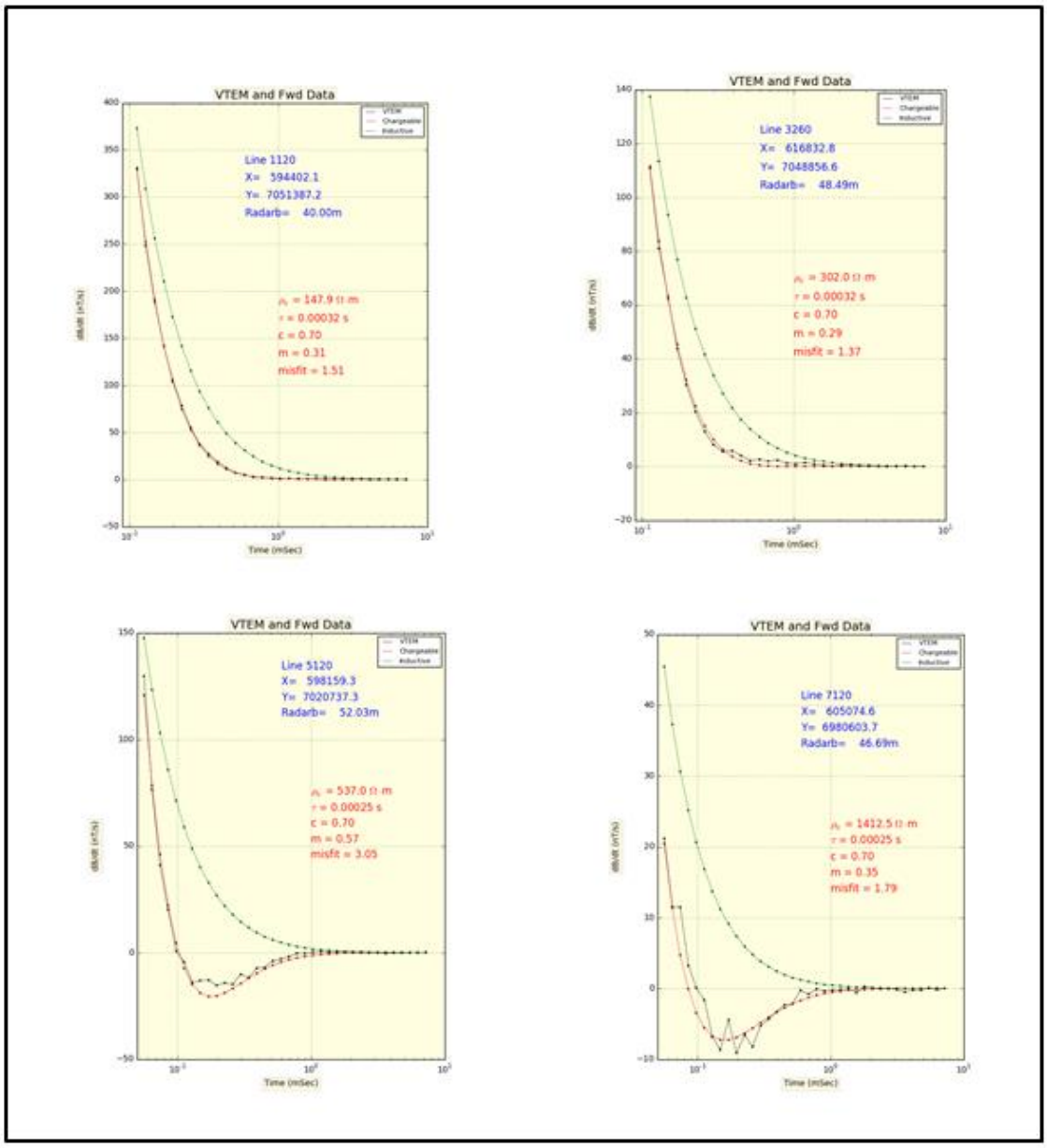

Figure 5: Cole-Cole parameters of four AIIP forward models and corresponding decays; purely inductive m=0 (green), observed data (black) and forward modeled data (red).

Typical Cole-Cole spectra for c=0.7 is shown in Figure 6. The width of the phase curve depends on c. For large c, the grain sizes of the polarizable material are distributed in a narrow range (or more uniformly distributed). The peak of the phase curve is related to the IP relaxation time-constant τ, or the average grain size of the polarizable materials.

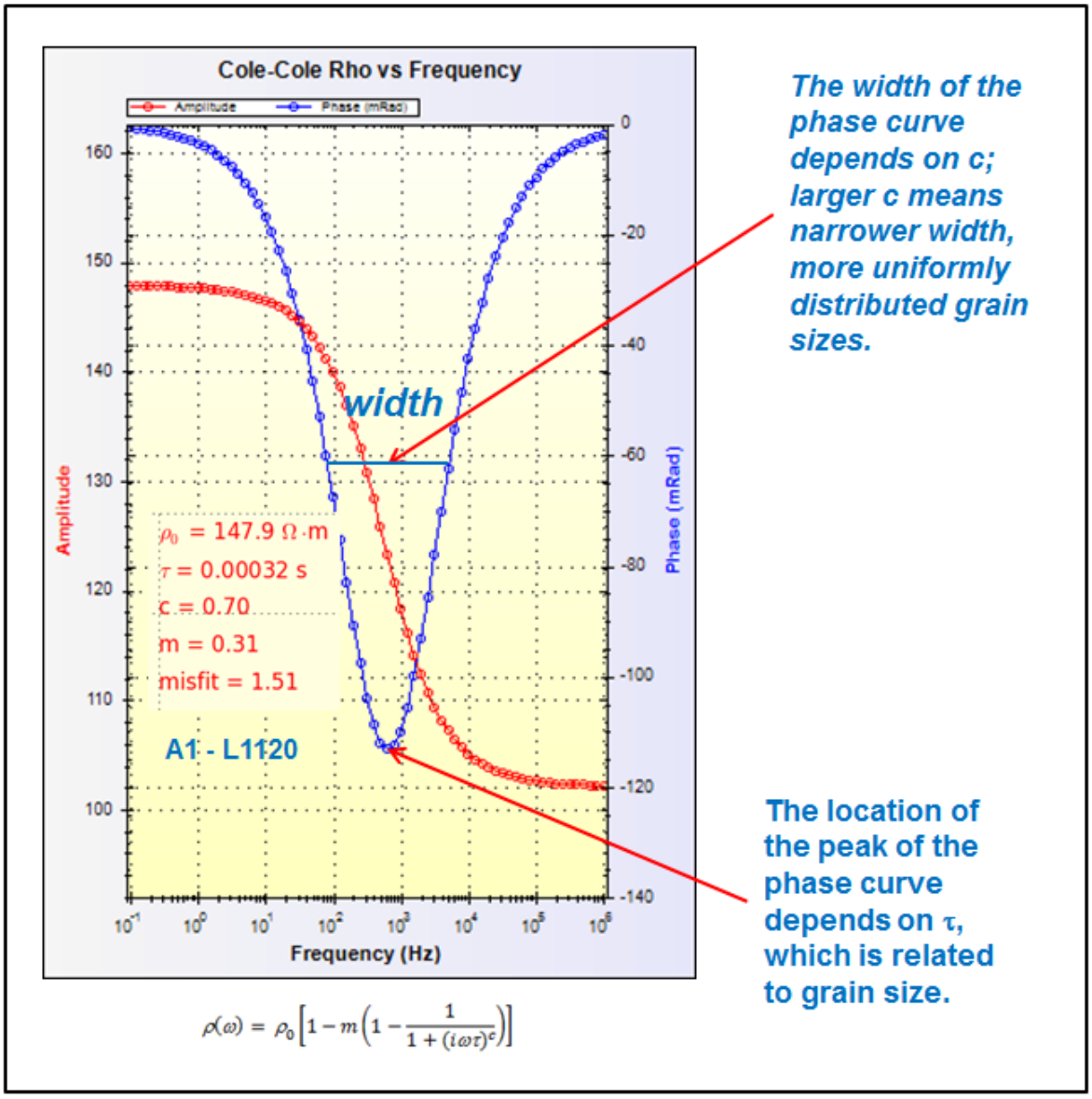

Figure 6: The relationship between the distribution of grain sizes and the frequency factor c is illustrated in the Cole-Cole spectra of c=0.7.

2.4 AIIP DEPTH OF INVESTIGATION

Using a buried chargeable prism in a uniform, non-polarizable ground, the depth of investigation of AIIP is studied. A 200 m by 200 m by 20 m prism of resistivity $\rho_1 = 10\,\Omega\cdot m$, $m = 0.5$ v/v, $\tau = 0.0002s$ *and* $c = 0.7$ is placed at various depths below ground in a resistive half space of resistivity $\rho_0 = 1{,}000\,\Omega\cdot m$, Figure 7. The size of the prism is within the footprint of the VTEM system, and the ground in the south of Coffee Road Property (A3 and A4) is quite resistive.

The software MarcoAir (CSIRO/AMIRA, Xiong and Tripp 1995) is used to generate the synthetic VTEM data in the AIIP depth of investigation. MarcoAir computes the airborne electromagnetic responses for prisms in layered earth. The Cole-Cole relaxation model is incorporated in MarcoAir.

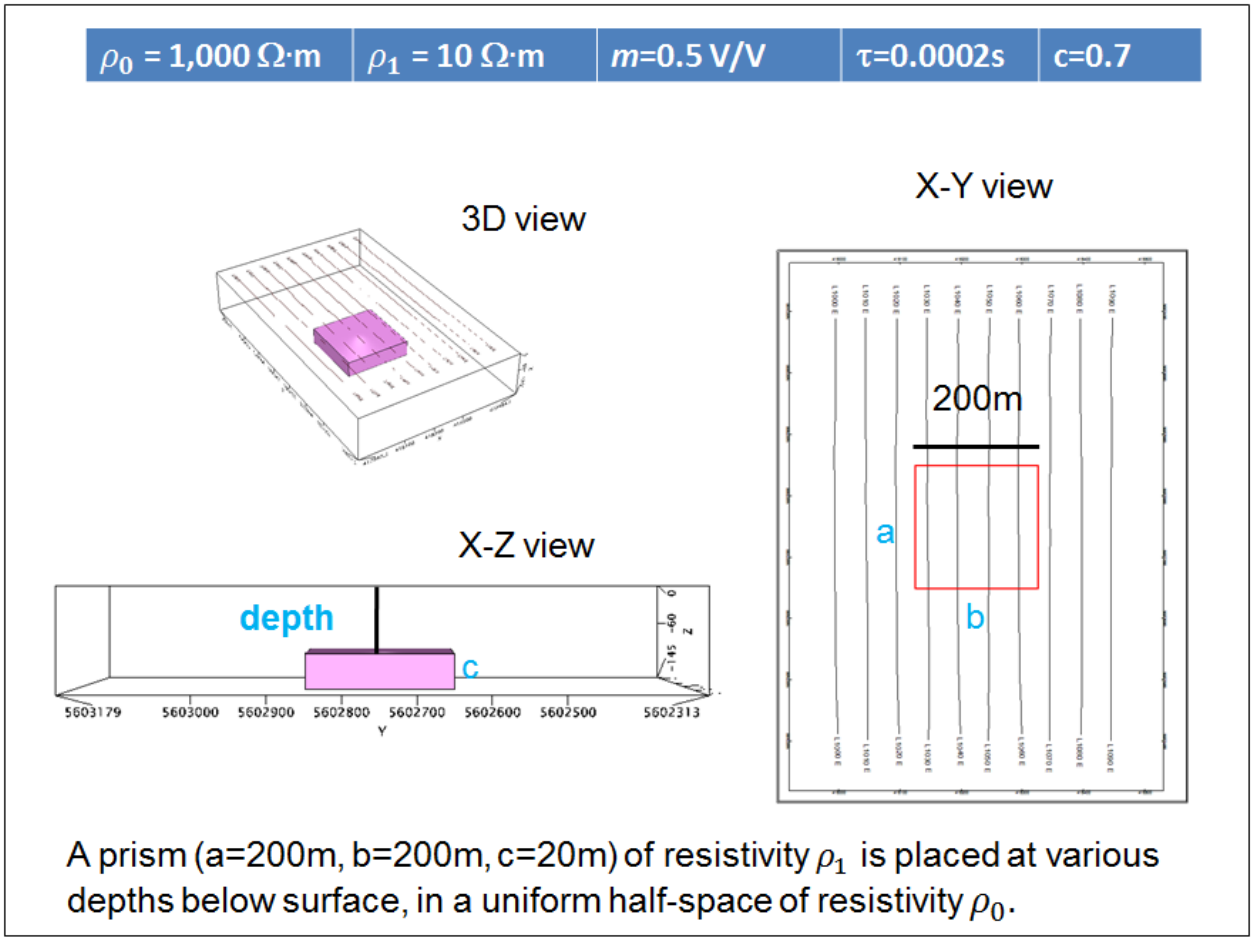

Figure 7: The setup of the 3D prismatic model for AIIP depth of investigation.

The AIIP apparent chargeability maps for the prisms buried at 50m, 75m and 100m depths are shown in Figure 8.

For the case of 50m deep prism, the maximum value of the recovered AIIP apparent chargeability is 0.58 V/V. The maximum recovered AIIP apparent chargeability for the 75m deep prism is 0.39 V/V. At 100m depth, maximum recovered AIIP apparent chargeability is 0.28 V/V, and the prism can still be detected and mapped by the VTEM system.

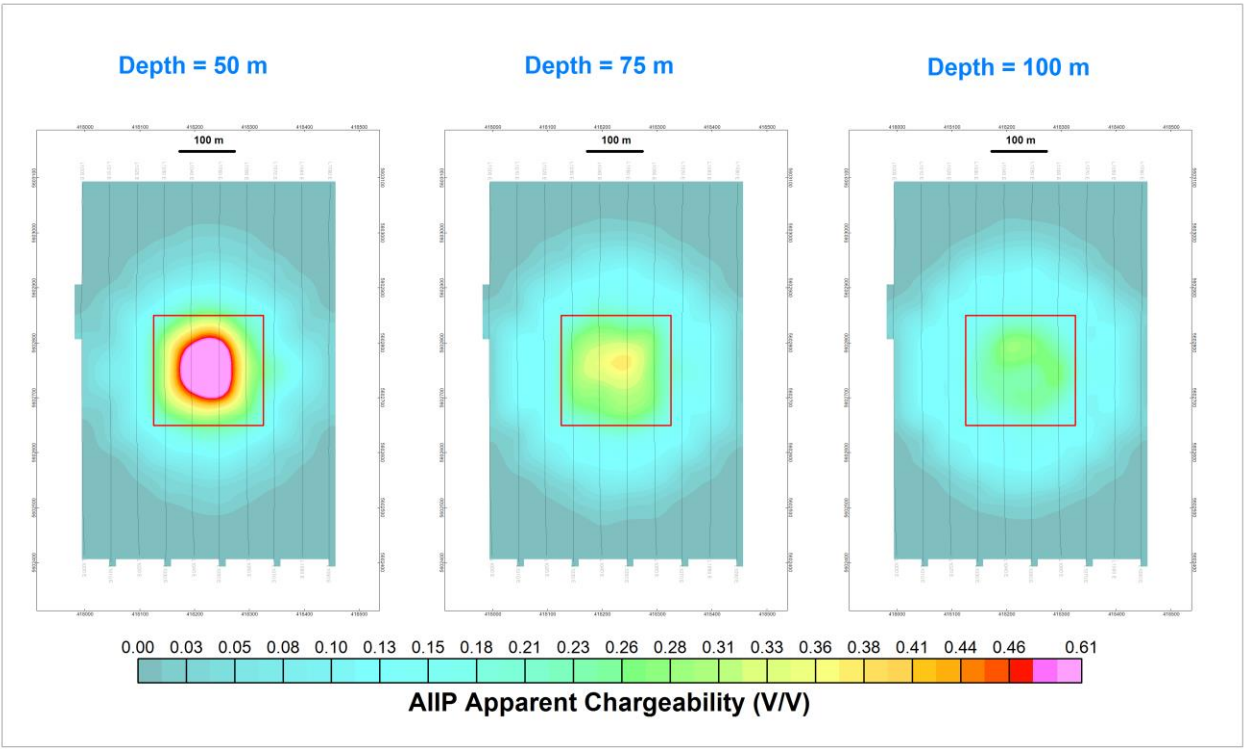

Figure 8: AIIP apparent chargeabilities for prisms located 50m, 75m and 100m below ground; the same color scheme is used.

The AIIP apparent resistivity maps for the prisms buried at 50m, 75m and 100m depths are shown in Figure 9.

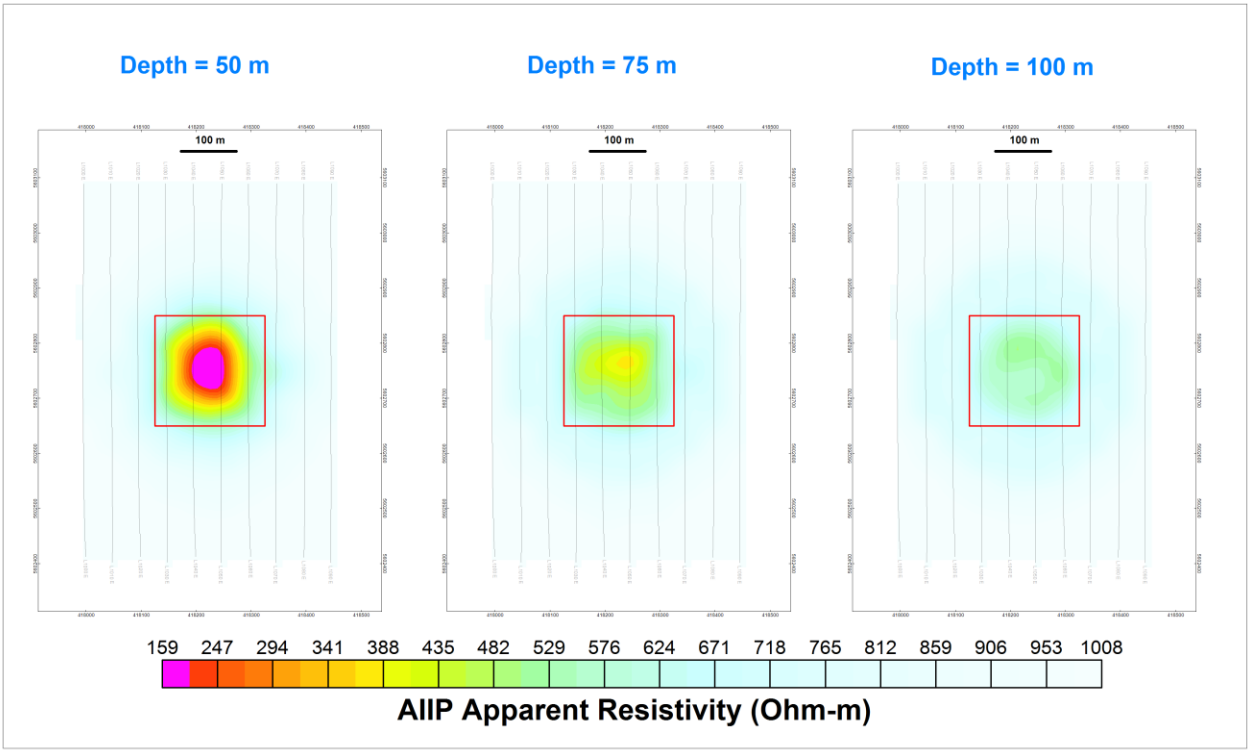

Figure 9: AIIP apparent resistivities for prisms located 50m, 75m and 100m below ground; the same color scheme is used.

At 100m depth in a resistive (1000 Ohm-m) host, a moderately chargeable prism may still be detectable by VTEM system, and the apparent chargeability (albeit weak) and resistivity recovered by AIIP mapping, as illustrated in Figure 10. Again, the expression of the AIIP effect in VTEM data is the distortion of the decay curve. Negative transient is not required to prove the existence of AIIP effect in VTEM data.

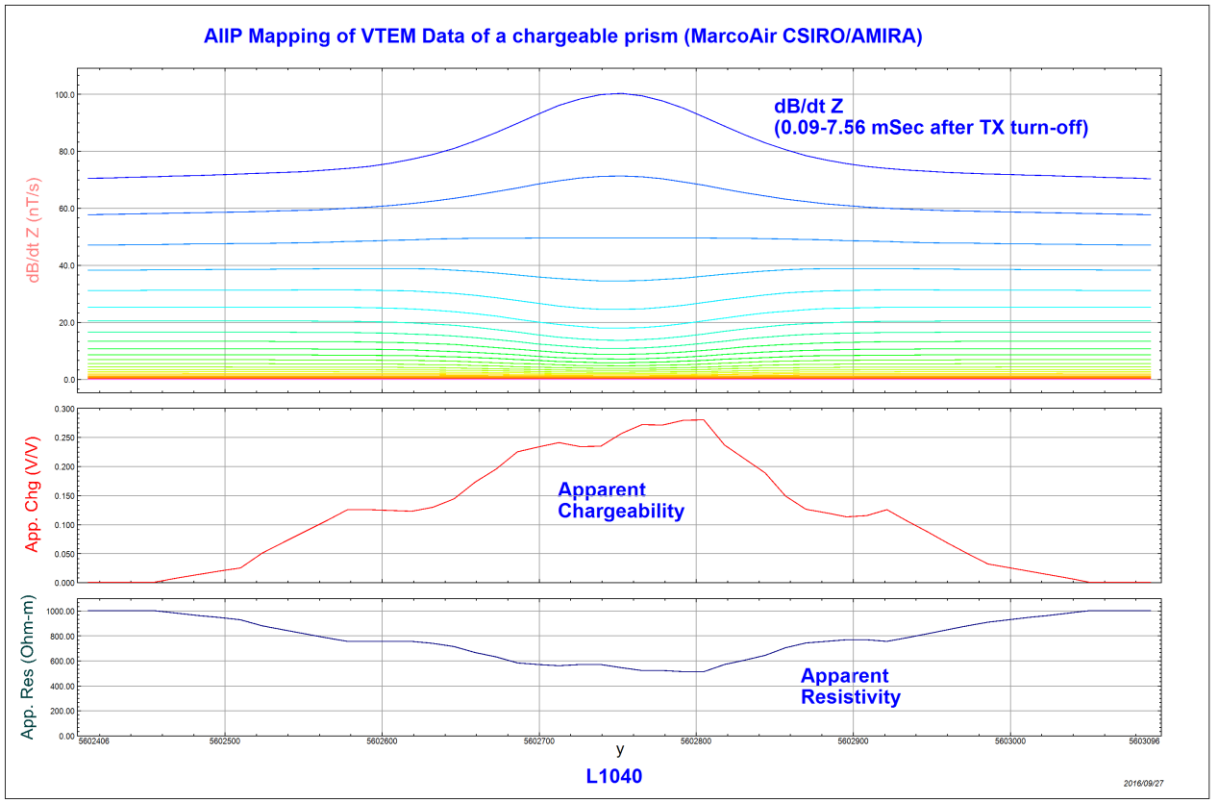

Figure 10: Forward modeled VTEM data of a chargeable prism at 100m depth, and recovered apparent chargeability and resistivity, synthetic line L1040 (just left of the prism centre).

3. AIIP CHARGEABILITY MAPPING RESULTS

3.1 GEOLOGY AND KNOWN GOLD MINERALIZATION

The discussions of the geology of the Coffee Road property are based mainly on the work by MacKenzie, Craw & Finnigan., 2014.

The basement of the Coffee Road property consists of the Paleozoic metamorphic rocks of the Yukon Tanana Terrane (YTT), Figure 11, Mackenzie, Craw & Finnigan, 2014. The basement rocks of VTEM areas A1, A3, A4 and western half of A5 are mainly undifferentiated schist and gneiss, and the basement of areas A2 and eastern half of A5 comprises mainly of Late Permian granitoid.

The basement rocks were deformed, folded and stacked during the Jurassic along regional-scale thrust faults. Greenschist facies shear zones and alteration developed during this time. Later stages of more brittle folding and fracturing subsequently developed and were locally infilled by orogenic quartz veins formed from fluids generated at depth within the thickened metamorphic pile. Hydrothermal alteration and disseminated gold mineralization in the White Gold District located just west of the Coffee Road property are structurally controlled by extensional fractures and EW striking Jurassic faults and shear zones, Mackenzie, Craw & Finnigan, 2014.

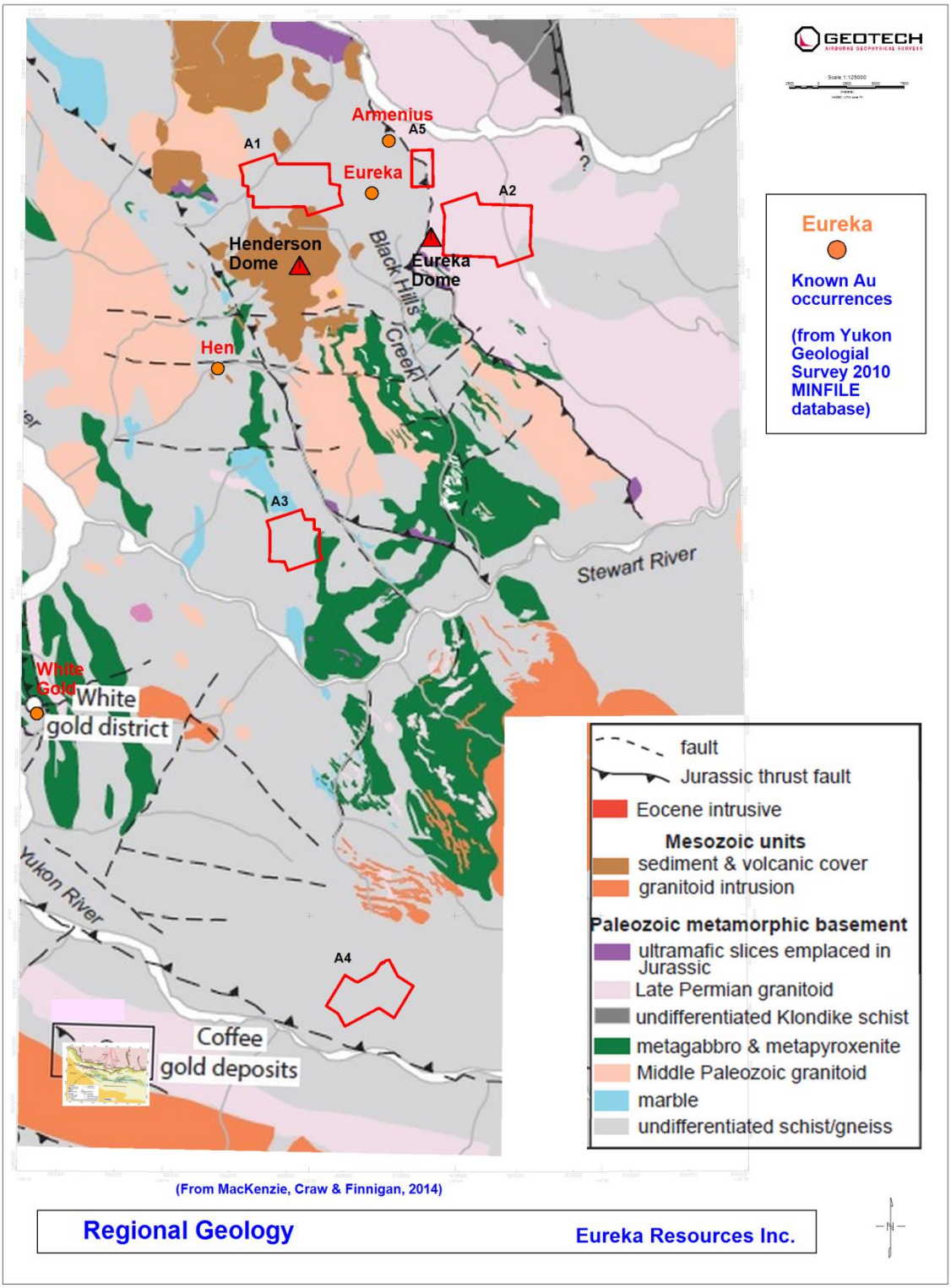

Figure 11: Regional geology of the Coffee Road Property, from MacKenzie, Craw & Finnigan, 2014, three known gold occurrences, i.e., Armenius, Eureka & Hen (from Yukon Geological Survey 2010 and appeared in Chapman et al., 2011) and the Coffee gold deposits (from Bultenhuis, Boyce & Finnigan, 2015) located west and southwest of A4.

Chapman, Mortensen & LeBarge, 2011 concluded that the placer gold deposits of the Indian River and Black Hills Creek (A1, A2 & A5) had formed mainly as a consequence of erosion of orogenic gold mineralization.

Bailey, 2013 proposed a Jurassic orogenic gold mineralization model for the Golden Saddle gold deposit, west and southwest of A3, in the White Gold District.

The Coffee deposits, west and southwest of A4, represent the shallower epizonal extensions of the mesozonal orogenic mineralization at the Boulevard deposit, a Cretaceous orogenic gold deposit, to the south (Buitenhuis, Boyce & Finnigan, 2015).

3.2 MAGNETIC DATA

Potential orogenic gold mineralization in the Coffee Road property is likely to be controlled by local scale geological structures such as fractures or faults, which can be mapped by the magnetic data.

The interpreted structures, i.e., faults, and possible thrusts and intrusions over the Calculated Vertical Gradient (CVG) data of the VTEM areas are shown in Figure 12.

The inferred faults may act as conduits or pathways for possible metamorphic or hydrothermal fluids, leading to possible hydrothermal alteration or even gold mineralization in host rocks.

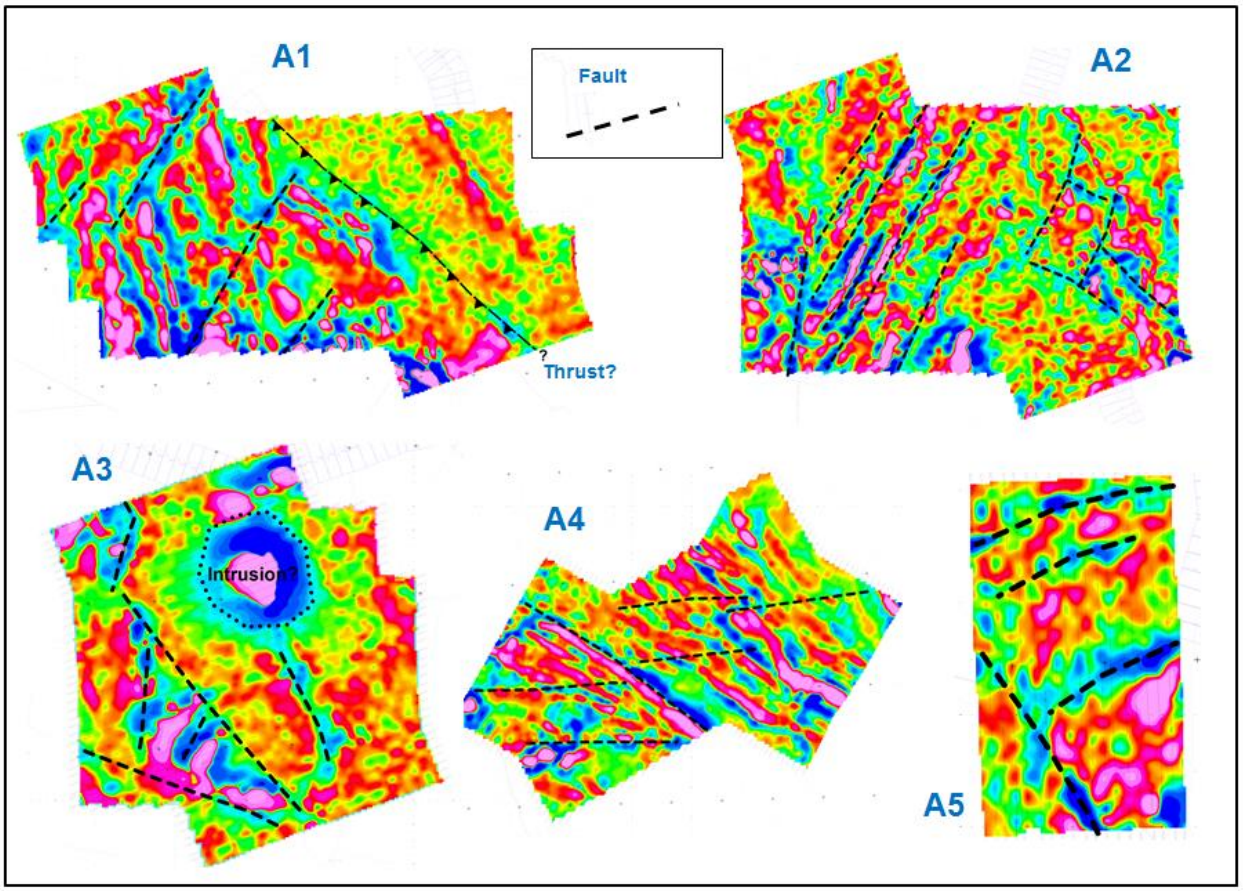

Figure 12: Inferred faults and possible thrust (A1) and intrusion (A3) over the CVG data of VTEM areas.

3.3 AIIP MAPS AND POTENTIAL GOLD PROSPECTS

The AIIP apparent chargeability and resistivity maps derived using frequency factor c of 0.7 of A1 block are shown in Figure 13. The strong conductive and chargeable zones don't appear to be coinciding with the drainages, implying that the conductive and chargeable materials are located within the hard rocks. The AIIP anomalies could be related to the fault zones, which acted as conduits for hydrothermal or metamorphic fluids possibly carrying sulphide minerals and even gold. The AIIP conductive and chargeable zones are selected as potential orogenic gold exploration prospects.

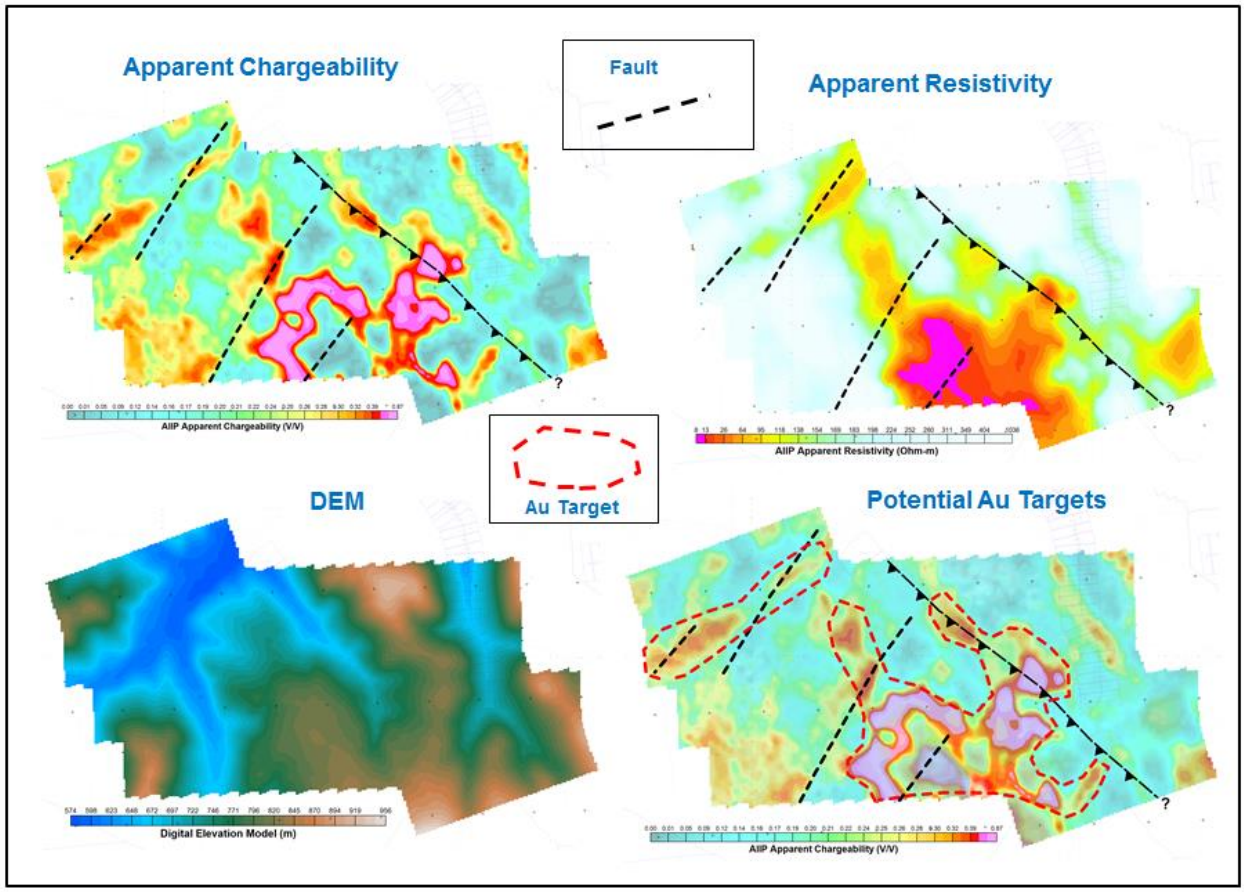

Figure 13: AIIP apparent chargeability, resistivity maps, DEM and potential gold targets, A1 block.

The AIIP apparent chargeability and resistivity maps of A2 block are shown in Figure 14. It appears that the conductive zones follow more or less the drainages. However, the chargeable anomalies in the west of the block don't appear to be related to drainages. These chargeable anomalies could be related to the NE-SW trending inferred faults in the same area. A potential orogenic gold exploration prospect for A2 is identified and shown over the AIIP apparent chargeability.

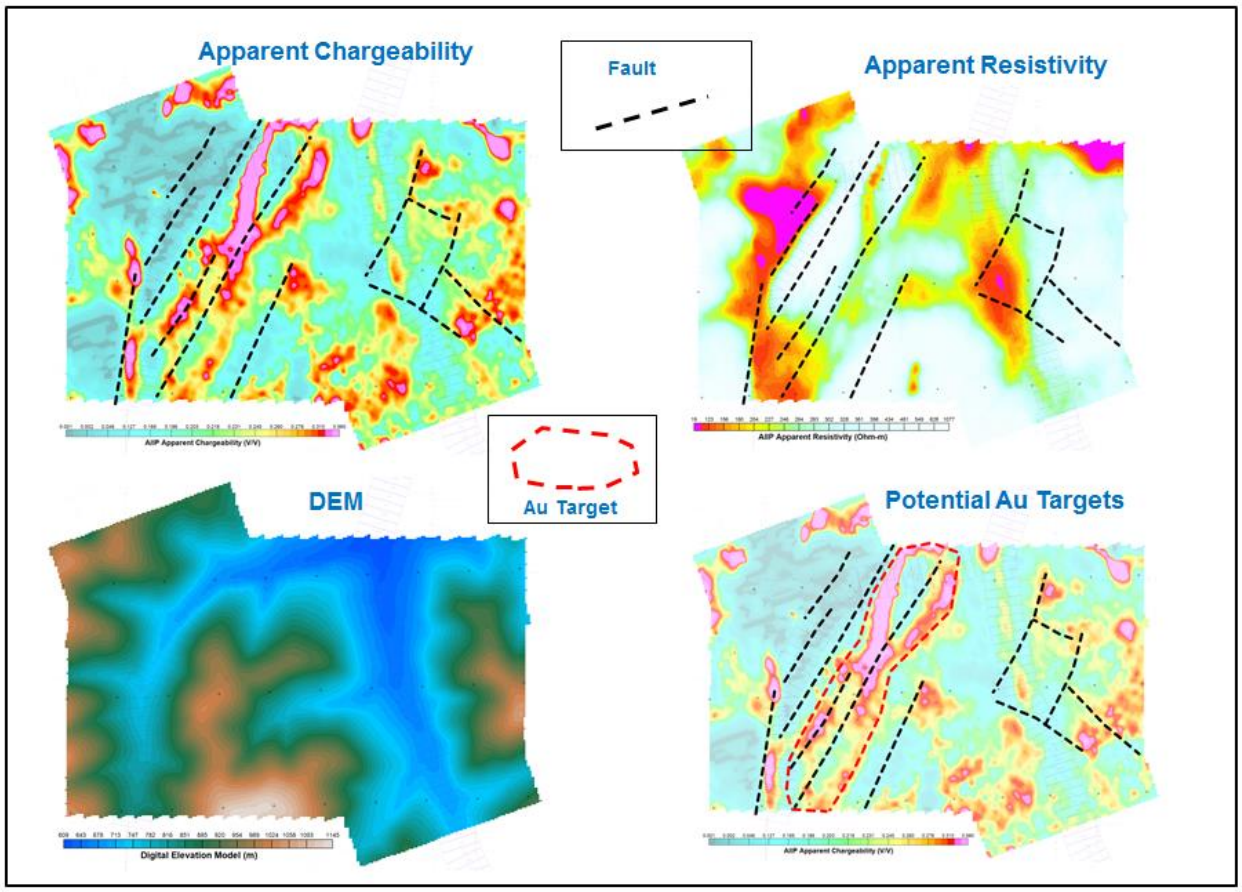

Figure 14: AIIP apparent chargeability, resistivity maps, DEM and potential gold targets, A2 block.

The AIIP apparent chargeability and resistivity maps of A3 block are shown in Figure 15. It appears that the AIIP anomalies do not follow the drainages. The chargeable anomalies are located within resistive terrains, implying that they could be possibly related to sulphide mineralization in quartz veins. A potential gold exploration prospect in the western half of A3 block is outlined and displayed over the AIIP apparent chargeability.

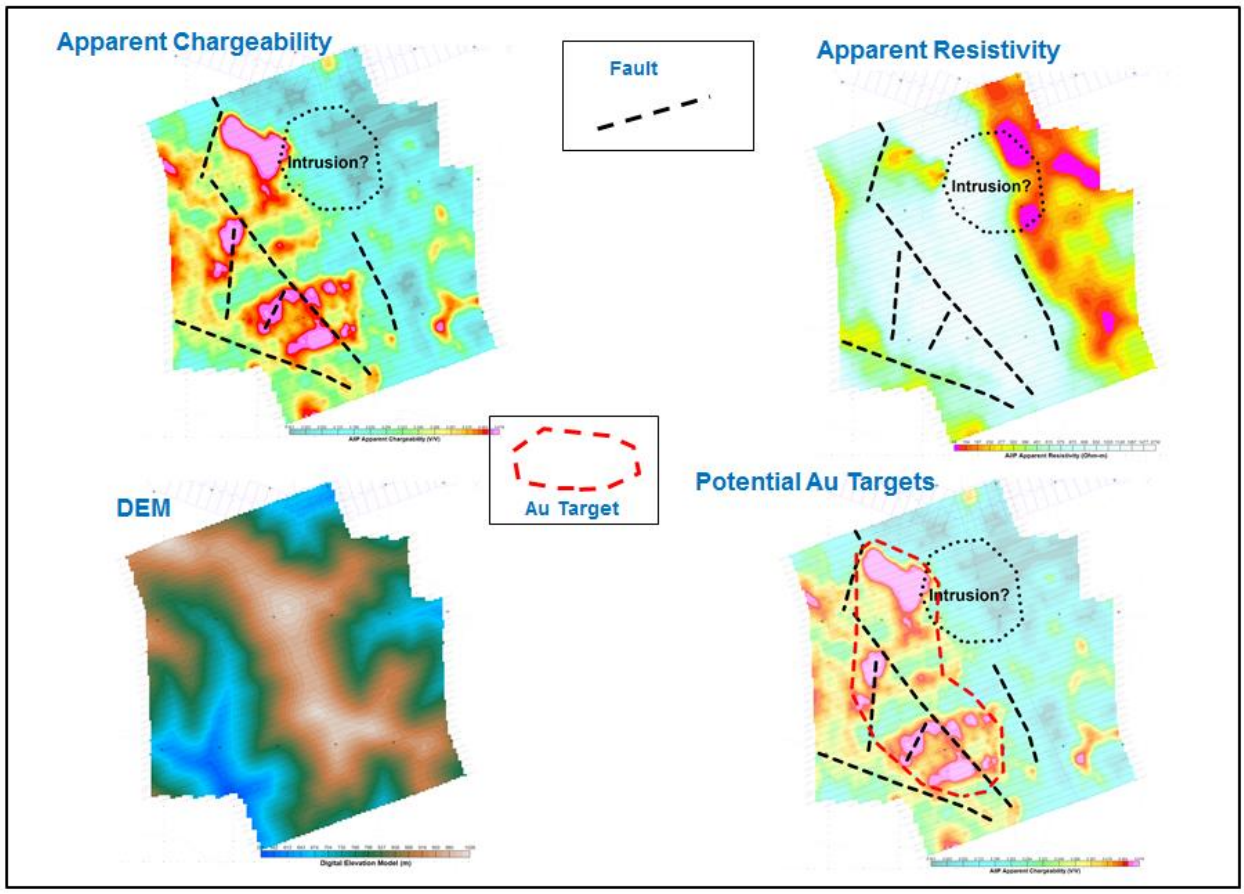

Figure 15: AIIP apparent chargeability, resistivity maps, DEM and potential gold targets, A3 block.

The AIIP apparent chargeability and resistivity maps of A4 block are shown in Figure 16. It appears that the AIIP apparent chargeability anomalies do not follow the drainages, but the AIIP apparent resistivity anomalies appear to follow the drainages closely in the SW portion of A4. The chargeable anomalies are located within resistive terrains in the NE of A4, implying that they could be possibly related to sulphide mineralization in quartz veins. The chargeable anomalies seem to trend parallel to the inferred faults. A potential gold exploration prospect in A4 block is identified and displayed over the AIIP apparent chargeability.

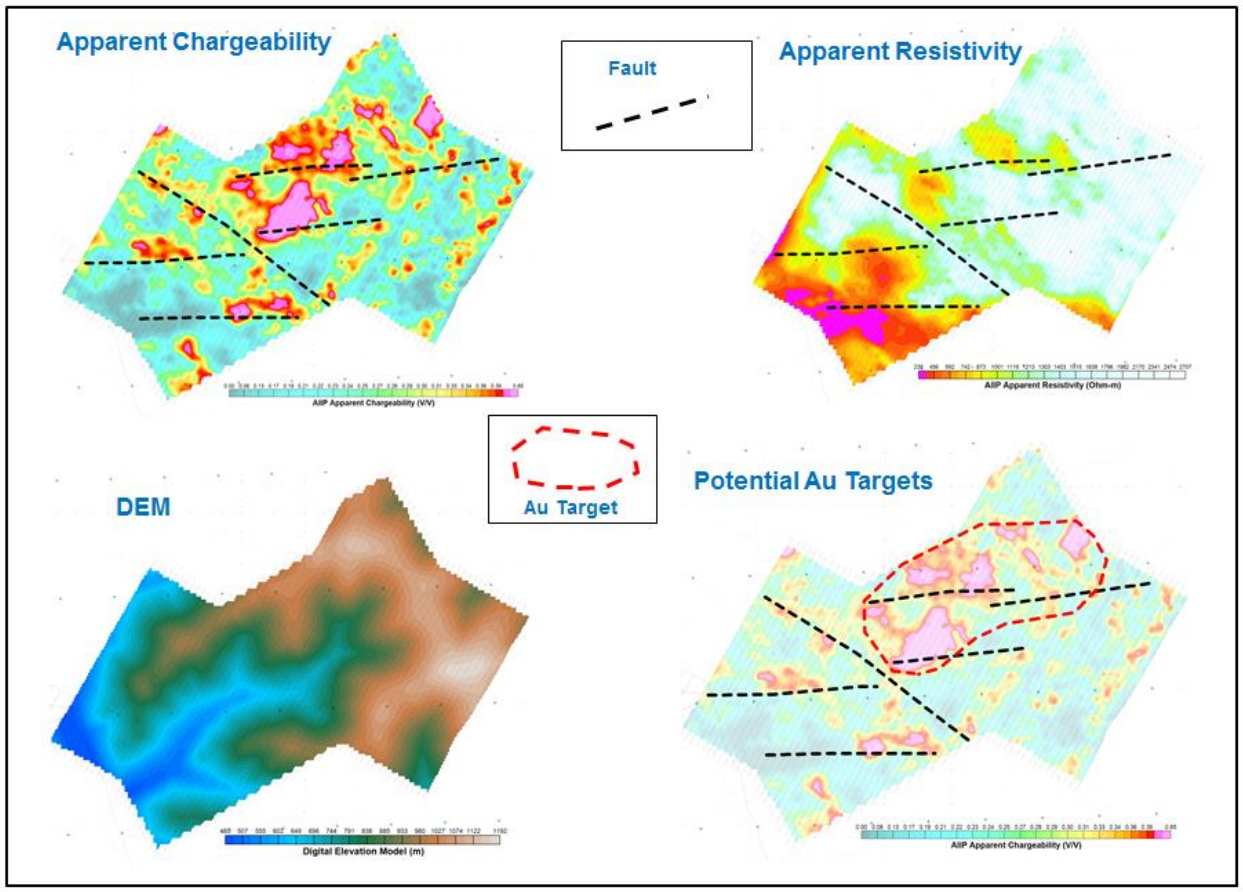

Figure 16: AIIP apparent chargeability, resistivity maps, DEM and potential gold targets, A4 block.

The AIIP apparent chargeability and resistivity maps of A5 block are shown in Figure 17. It appears that the AIIP anomalies don't follow the drainages. The chargeable anomalies in the south of the block are located in resistive terrains and they could be related to sulphides in quartz veins. The chargeable anomalies in the north are located very close to the central conductive zone, which is trending ENE direction and fairly conductive. The central conductive zone could be related to possible massive sulphide mineralization. Potential gold exploration prospects for A5 are identified and shown over the AIIP apparent chargeability.

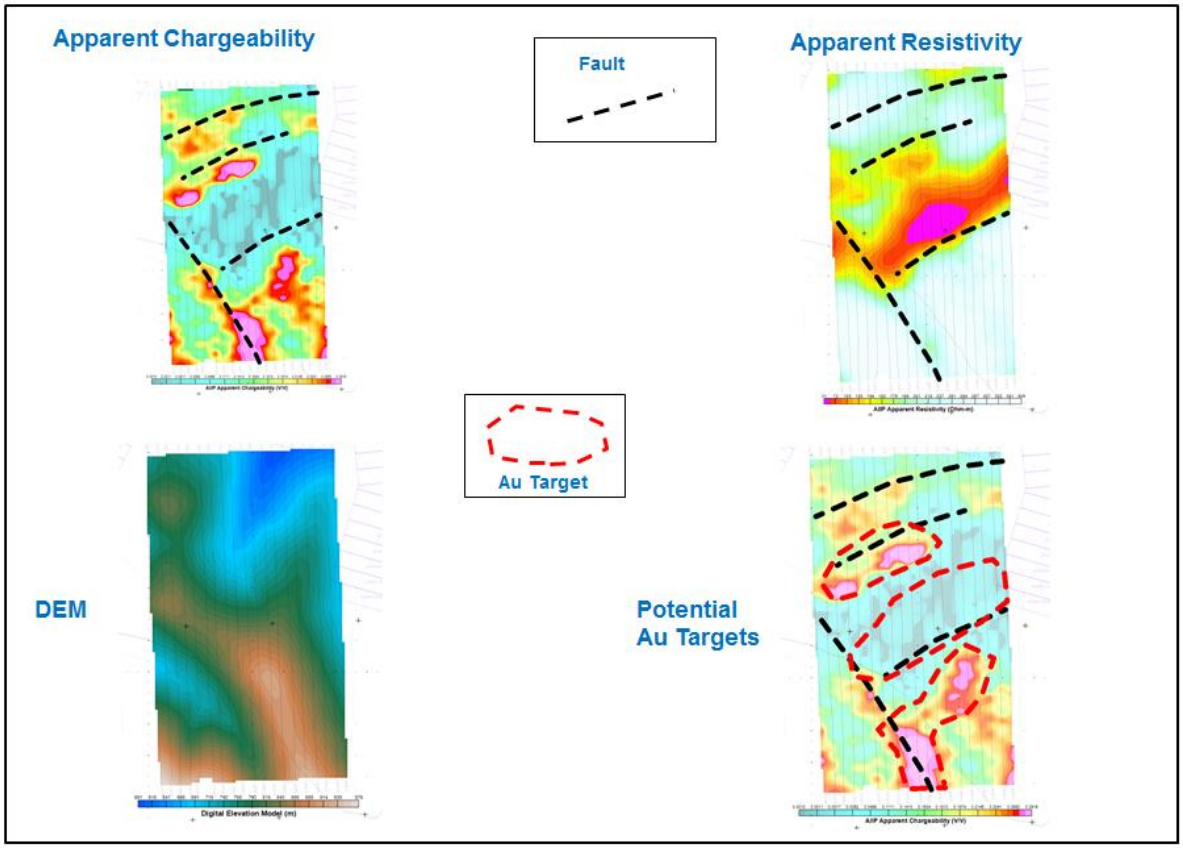

Figure 17: AIIP apparent chargeability, resistivity maps, DEM and potential gold targets, A5 block.

3.4 DISCUSSIONS OF AIIP SOURCES

The following discussions focus on the possible sources of AIIP and implications for the exploration of potential orogenic gold mineralization in the VTEM blocks.

There are three main sources of orogenic gold (Augustin & Gaboury, 2017 and references therein):

1. Intrusion-related sources (e.g. Porphyries);
2. Carbonaceous, pyrite-rich sedimentary rocks (Large *et al.*, 2011);
3. Plume-related basaltic rocks (Bierlein & Pisarevsky, 2008);

The first two possible sources of gold could be present in the VTEM blocks.

The majority of orogenic gold deposits formed proximal to regional terrane-boundary structures that acted as vertically extensive hydrothermal plumbing systems, and most deposits are sited in second or third order splays or fault intersections that define domains of low mean stress and correspondingly high fluid fluxes, McCuaig and Kerrich 1998.

The origin of gold in some types of orogenic gold deposits, such as turbidite-hosted, or sediment-hosted gold deposits, is an active research topic. Some of the conventional beliefs and new ideas

from Large *et al*., 2011 regarding the carbonaceous pyrite-rich sedimentary source of gold for these deposits are listed below, representing two different theories. In either case, structure, i.e., fault, and hydrothermal activity are two of the most critical factors in the formation of the gold deposits.

Conventional Beliefs	***New Ideas (Large et al., 2011)***
Gold is coming from some deep sources or from crustal granite	Gold is already present in the sedimentary basin
Graphitic sediments are good trap rocks for gold	Graphitic sediments are ideal source rocks for Au & As and other trace elements
Gold is introduced late; i.e., syn-tectonic or post-tectonic	Gold is introduced early; i.e., pre-tectonic and moved around late during tectonism

Some AIIP results have indicated that some hydrothermal alteration products, i.e., hydrothermal pyrite, can generate conductive and chargeable responses in VTEM data. The linear conductive and chargeable trends tend to coincide with or to be locaed in close proximity to fault zones, which acted as conduits for hydrothermal or metamorphic fluids.

The hydrothermal alteration assemblages, i.e., sericitization, carbonatization, sulphidation (pyrite) and etc., are common to many orogenic gold deposits, Bierlein *et al*., 2000, and the recognition of extensive alteration halos around them, especially hydrothermal pyrites, by AIIP mapping represents a potentially powerful tool for gold exploration.

The hydrothermal alteration products in general are fine-grained.

4. CONCLUSIONS AND RECOMMENDATIONS

The AIIP chargeability mapping of VTEM data from the A1-Ophir, A2-Sheba, A3-Hav, A4-Tak, and A5-Etta blocks located within the Coffee Road Property, Yukon, has been carried out.

Potential exploration prospects for orogenic gold mineralization in the blocks are identified and they are recommended for follow-up.

Respectfully submitted,

_____

Karl Kwan, M.Sc. P.Geo. (Limited[2])
Senior Geophysicist/Interpreter

_____ _____

Alexander Prikhodko, Ph.D., P.Geo.
Geophysical Director

Geoffrey Plastow, P.Geo.
Data Processing Manager

Geotech Ltd.
September 20, 2017

[2] The designation of P.Geo (Limited) by Association of Professional Geoscientists of Ontario permits the principal interpreter to practice in the field of exploration geophysics only.

ACKNOWLEDGEMENTS

The AIIP chargeability mapping algorithm, developed by Geotech, is based on Airbeo (CSIRO/AMIRA), which is part of a suite of software of project P223F released to the public in 2010 by CSIRO/AMIRA.

REFERENCES

Augustin, Jérôme and Gaboury, Damien, 2017: Paleoproterozoic plume-related basaltic rocks in the Mana gold district in western Burkina Faso, West Africa: Implications for exploration and the source of gold in orogenic deposits, Journal of African Earth Sciences, **129**, 17-30.

Bailey, Leif Anthony, 2013: Late Jurassic fault-hosted gold mineralization of the Golden Saddle Deposit, White Gold District, Yukon Territory, M.Sc. thesis, The University of British Columbia.

Bierlein, Frank P. and Pisarevsky, S., 2008: Plume-related oceanic plateaus as a potential source of gold mineralization, **103**, 425-430.

Bierlein, F.P., Arne, D.C., McKnight, S., Lu, J., Reeves. S., Besanko, J, Marek, J., and Cooke, D., 2000: Wall-rock petrology and geochemistry in alteration halos associated with mesothermal gold mineralization, Central Victoria, Australia, Economic Geology, **95**, 283-312.

Buitenhuis, E., Boyce, L. and Finnigan, C., 2015: Advances in the mineralization styles and petrogenesis of the Coffee gold deposit, Yukon. *In:* Yukon Exploration and Geology 2014, K.E. MacFarlane, M.G. Nordling and P.J. Sack (eds.), Yukon Geological Survey, p. 29-43.

Chapman, Robert John, Mortensen, James Keith and LeBarge, William P., 2011: Styles of lode gold mineralization contributing to the placers of the Indian River and Black Hills Creek, Yukon Territory, Canada as deduced from microchemical characterization of placer gold grains, Miner Deposita, **46**, 881-903.

Chen, J., and Raiche, A., 1998: Inverting AEM data using a damped eigenparameter method: Exploration Geophysics, **29**, 128–132.

Cole, K. and Cole R., 1941: Dispersion and absorption in dielectrics, Part I. Alternating current characteristics: Journal of Chemical Physics, **9**, 341-351.

Goldfarb, Richard J. and Groves, David I., 2015: Orogenic gold: Common or evolving fluid and metal sources through time, Lithos**, 233**, 2-26.

Groves, D.I., Goldfarb, R.J., Gebre-Mariam, M., Hagemann, S.G. and Robert F., 1998, Orogenic gold deposits: A proposed classification in the context of their crustal distribution and relationship to other gold deposit types, Ore Geology Reviews, **13**, 7-27.

Kratzer, T. and Macnae, J.C., 2012: Induced polarization in airborne EM, Geophysics, **77**, E317-327.

Kwan, K., Prikhodko, A., Legault, Jean M., Plastow, G., Xie, J. and Fisk, K., 2015a: Airborne Inductive Induced Polarization Chargeability Mapping of VTEM data, ASEG-PESA 24th International Geophysical Conference and Exhibition, Perth, Australia.

Kwan, K., Prikhodko, A. and Legault, J.M., 2015b: Airborne inductively induced polarization effects in and their removal from the VTEM data from Mirny, Russia, Extended Abstract, SEG New Orleans 2015 International Exposition and 85th Annual Meeting.

Large, Ross R., Bull, Stuart W. and Maslennikov, Valeriy, 2011: A carbonaceous sedimentary source-rock model for Carlin-type and orogenic gold deposits, Economic Geology, **106**, 331-358.

Luo Y. and Zhang G. 1998: Theory and application of Spectral Induced Polarization, Geophysical Monograph Series.

MacKenzie, D., Craw, D., and Finnigan, C., 2014: Structural controls on alteration and mineralization at the Coffee gold deposits, Yukon. *In:* Yukon Exploration and Geology 2013, K.E. MacFarlane, M.G. Nordling, and P.J. Sack (eds.), Yukon Geological Survey, p. 119-131.

McCuaig, T. Campbell and Kerrich, Robert, 1998: P-T-t-deformation-fluid characteristics of lode gold deposits: evidence from alteration systematics, Ore Geology Reviews, **12**, 381-453.

Nelder, J.A., and Mead, R, 1965: A Simplex Method for Function Minimization, *Computer Journal*, **7** (4), 308-313.

Pelton, W.H., Ward, S.H., Hallof, P.G., Sill, W.R., and Nelson, P.H., 1978, Mineral discrimination and removal of inductive coupling with multi-frequency IP: Geophysics, **43**, 588–609.

Raiche, A., 1998: Modelling the time-domain response of AEM systems: Exploration Geophysics, **29**, 103–106.

Robert, F., Brommecker, R., Bourne, B. T., Dobak, P.J., McEwan, C. J., Row, R.R. and Zhou, X., 2007: Models and exploration methods for major gold deposit types, in "Proceedings of Exploration 07: Fifth Decennial International Conference on Mineral Exploration", Edited by B. Milkereit, 691-711.

Weidelt, P., 1982: Response characteristics of coincident loop transient electromagnetic systems, Geophysics, **47**, 9, 1325-1330.

Wong, J., 1979. An electrochemical model of the induced polarization phenomenon in disseminated sulfide ores: Geophysics, **44**, 1245-1265.

Xiong, Zonghou and Tripp, Alan C., 1995: A block iterative algorithm for 3-D electromagnetic modeling using integral equations with symmetrized substructures, Geophysics, 60, 1, 291-295.

Yukon Geological Survey, 2010: Yukon mineral occurrence database.

APPENDIX A: AIIP Mapping

INTRODUCTION

Data acquired by airborne in-loop time-domain electromagnetic (EM) systems, such as VTEM™ (Witherly et al., 2004), reflect mainly two physical phenomena in the earth: (1) EM induction, related to ground conductivity, (2) Airborne Inductively Induced Polarization (AIIP), related to the relaxation of polarized charges in the ground (e.g., Kratzer & Macnae 2012 and Kwan *et al*., 2015).

It has been shown by Smith and West (1989) that the in-loop EM system is optimally configured to excite a unique AIIP response, including negative transients in mid to late times over resistive grounds, from bodies of modest chargeability.

Negative transients observed in airborne time domain EM data (e.g. Smith and Klein, 1996 and Boyko et al. 2001) are attributed to airborne inductive induced polarization (AIIP) effects. However, the absence of negative transients does not preclude the presence of AIIP, because of the IP effect takes finite time to build up or the IP effect may be obscured by the conductive ground (Kratzer and Macnae, 2012).

In mineral exploration, near-surface sources of AIIP are clays through membrane polarization (electrical energy stored at boundary layer) and most metallic sulphides and graphite through electrode polarization (electrical charges accumulated through electrochemical diffusion at ionic-electronic conduction interfaces). Some kimberlites in Lac de Gras kimberlite field are known to have AIIP signatures (Boyko *et al*., 2001).

The widely used theory to explain the IP effect is the empirical Cole-Cole relaxation model (Cole and Cole, 1941) for frequency dependent resistivity $\rho(\omega)$,

$$\rho(\omega) = \rho_0 \left[1 - m\left(1 - \frac{1}{1+(i\omega\tau)^c}\right)\right], \quad (1)$$

where ρ_0 is the low frequency asymptotic resistivity, m is the chargeability, τ is the IP relaxation time constant, $w = 2\pi f$, and c is the frequency factor.

The extraction of AIIP chargeability m using the Cole-Cole formulation from VTEM data had been demonstrated by Kratzer and Macnae, 2012 and Kwan *et al*., 2015.

An improved version of AIIP chargeability mapping tool based on CSIRO/AMIRA Airbeo has been developed for VTEM system and tested on VTEM data from Mt Milligan, British Columbia, Canada, and Tullah, Tasmania.

IMPROVED AIIP MAPPING ALGORITHM

Search for *m* and τ using Airbeo forward modeling

The extraction of the four Cole-Cole parameters (ρ_0, m, τ and c) from airborne VTEM data can be a difficult task. The AIIP mapping algorithm originally developed by Kwan *et al*., 2015 suffers lack of precision for the derived apparent chargeability m and resistivity ρ_0, and is computationally very slow. Geotech has recently developed an improved version of AIIP mapping algorithm, based on Airbeo from CSIRO/AMIRA[1] (Chen & Raiche 1998; Raiche 1998) to extract the (ρ_0, m and τ) parameters while keeping the frequency factor c fixed. The new method applies the Nelder-Mead Simplex minimization (Nelder and Mead, 1965) in the two-dimensional (m,τ) plane. At each required test point (m_i, τ_i), the optimal background resistivity $\rho_0$is found by one-dimensional Golden Section minimization (Press *et al*., 2002). The algorithm uses only Airbeo's forward modeling kernel, which can generate synthetic VTEM data with high precision. The Nelder-Mead AIIP mapping algorithm generates much more precise (ρ_0, m, τ) parameters.

The Nelder-Mead Simplex Minimization method can be explained in the five (5) moves, reflection, expansion, outside and inside contraction, and shrink, as illustrated in Figure 1.

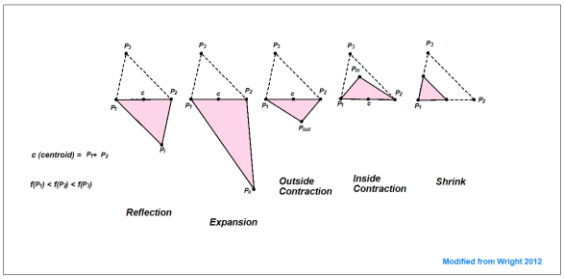

Figure 1: Nelder-Mead Simplex moves (modified from Wright 2012).

The Nelder-Mead Simplex minimization algorithm consists of following steps.

Let $f(\rho_0, m, \tau)$ be the RMS error function defined as

[1] Commonwealth Scientific and Industrial Research Organization and Amira International;

$$f(\rho_0, \mathrm{m}, \tau) = \frac{1}{N-1} \left(\sum_{i=0}^{N-1} (\mathrm{f}(\rho_0, \mathrm{m}, \tau, t_i) - v(t_i))^2\right)^{1/2}. \quad (2)$$

Step 1 (Sorting)

Sort the vertices such that f(P_1) < f(P_2) < f(P_3). Point P_1 is the best point, P_2 is the next-to-worst point and P_3 is the worst point;

Step 2 (Reflection)

Reflect the worst point P_3, through the centroid of (P_1 and P_2) to obtain the reflected point P_r, and evaluate f(P_r).

If (f(P_1) < f(P_r) < f(P_2)), then replace the worst point P_3 with the reflected point P_r, and go to Step 5.

Step 3 (Expansion)

If (f(P_r) < f(P_1)), then extend the reflected point P_r, further pass the average of P_1 and P_2, to point P_e, and evaluate f(P_e)

(a) If f(P_e) < f(P_r), then replace P_3 with P_e, and go to Step 5
(b) Otherwise, replace the worst point P_3 with the reflected point P_r, and go to Step 5

Step 4 (Contraction or Shrink)

If the inequalities of Step 2 and 3 are not satisfied, then it is certain that the reflected point P_r is worse than the next-to-worst point P_2, (f(P_r) > f(P_2)) and, a smaller value of f might be found between P_3 and P_r. So try to contract the worst point P_3, to a point P_c between P_3 and P_r and evaluate f(P_c);

The best distance along the line from P_3 to P_r can be difficult to determine. Typical values of P_c are one-quarter and three-quarter of the way from P_3 to P_r. These are call inside and outside contraction points P_{in} and P_{out};

(a) If min(f(P_{in}), f(P_{out})) < f(P_2), then replace P_3 with the contraction point P_{in} or P_{out}, and to Step 5.

(b) Otherwise shrink the simplex into the best point, P_1, and go to Step 5.

Step 5 (Convergence Check)

Stop if the standard deviation of *f* is less than user-specified tolerance *RMSTOL*,

$$\sqrt{\frac{1}{n}\sum_{i=0}^{n-1}(f_i - f_{avg})^2} \leq RMSTOL$$

Perhaps the most important feature in the Nelder-Mead simplex method is Step (4b), the shrink. It allows the shape of the simplex to "adapt itself to the local landscape", Nelder and Mead, 1965. In essence, all the moves in the Nelder-Mead (NM) Simplex method are designed to move away from the worst point.

Han and Neumann 2006 showed that the NM simplex method deteriorates when the number of parameters to be minimized (n) increases. For n=1 or 2, NM convergence is acceptable. As n≥3, NM convergence slows dramatically as N increases. Due to this reason, Geotech applies the NM method only in the 2D (m,τ) plane, to ensure convergence as well as that all the NM moves can be checked visually.

AIIP MAPPING RESULTS

Mt. Milligan, British Columbia, Canada

Mt. Milligan Cu-Au deposit is located within Early Mesozoic Quesnel Terrane that hosts a number of Cu-Au porphyry deposits, Oldenburg et al, 1997. The Mt. Milligan intrusive complex consists dominantly of monzonitic rocks, including the MBX and Southern Star (SS) zones, all which host mineralization at Mt. Milligan (Figure 2). Mineralization in both zones consists of pyrite, chalcopyrite and magnetite with bornite localized along intrusive-volcanic contacts (Terrane Minerals Corp. NI 43-101, 2007). Copper-gold mineralization is primarily associated with potassic alteration with both copper grade and alteration intensity decreasing outwards from the monzonite stocks. Pyrite content increases dramatically outward from the stocks where it occurs in association with propylitic alteration, which forms a halo around the potassic-altered rocks.

Helicopter-borne VTEM surveys, including a small survey over Mt. Milligan, were carried out from July 29th to November 1st, 2007, on behalf of GeoscienceBC as part of the QUEST project in central British Columbia. The data were released to the public by GeoscienceBC and can be downloaded from http://www.geosciencebc.com.

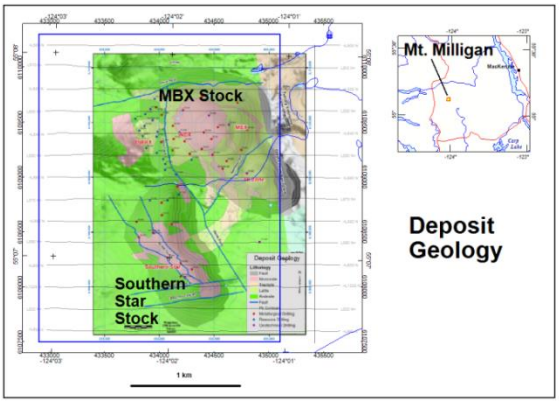

Figure 2: Mt. Milligan geology.

VTEM Z-component data, from 0.091 to 10.126 milliseconds in off-times, were processed to recover the AIP apparent chargeability. Very weak negative transients above noise level are observed in the VTEM data over two

locations from survey lines near DWBX and SS. The inverted Cole-Cole chargeabilities are shown in Figure 3. Weak chargeabilities can be seen along the east and west flanks of the MBX stock, especially over DWBX, and in a small area southwest of SS stock. For comparison, the chargeability slice at 40m depth, created by UBC 3D airborne IP inversion of the same VTEM data from Kang *et al*., 2014, is also shown.

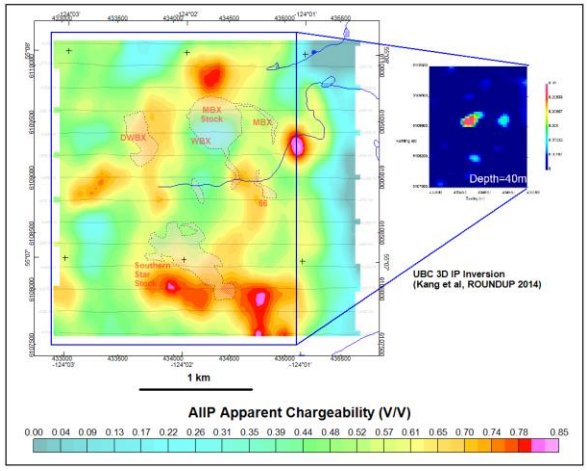

Figure 3: Mt. Milligan AIIP apparent chargeability.

The AIIP apparent resistivity of Mt. Milligan area is shown in Figure 4. A relatively low resistivity halo can be seen surrounding the SS stock.

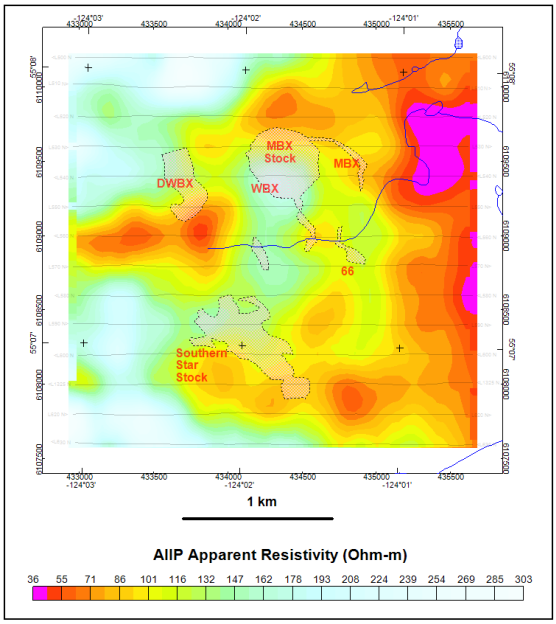

Figure 4: Mt. Milligan AIIP apparent resistivity.

Tullah, Tasmania

The most important metallogenic event in Tasmania occurred in Middle Cambrian as the post collisional proximal submarine volcanism and the deposition of the Mount Read Volcanics (MRV) and associated world-class deposits (Seymour *et al*., 2007).

The study area is located near Tullah, northwest Tasmania. The western half of the study area is covered by Late Cambrian quartz sandstone, Ordovician limestone and Quaternary alluvium and marine sediments (Figure). The eastern half is dominated by the Middle Cambrian volcanics (Corbett, 2002).

The Mount Lyell, located south of the study area, hosts 311 Mt 0.97% Cu and 0.31 g/t Au disseminated chalcopyrite-pyrite ore bodies in alteration assemblages of mainly quartz-sericite or quartz-chlorite-sericite.

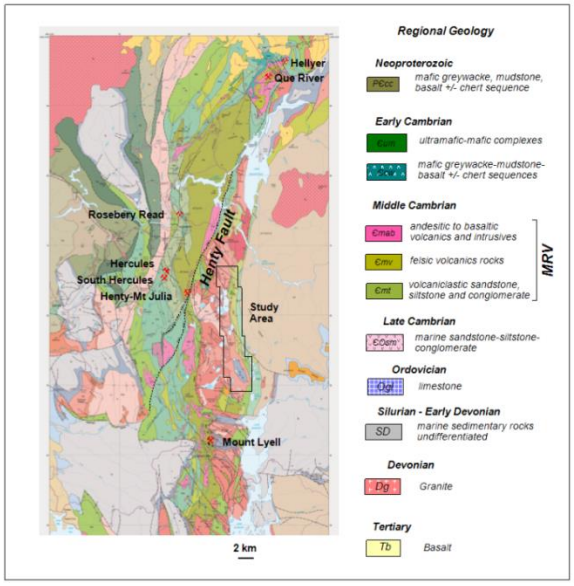

Figure 5: Regional geology of study area, Tullah, Tasmania.

From December 2012 to February 2013, Geotech carried out a helicopter-borne geophysical survey over the study area. Numerous negative transients were observed in the VTEM voltage data (Figure). The Z-component data, from 0.216 to 7.56 milliseconds in off-times, were processed for AIIP apparent chargeability.

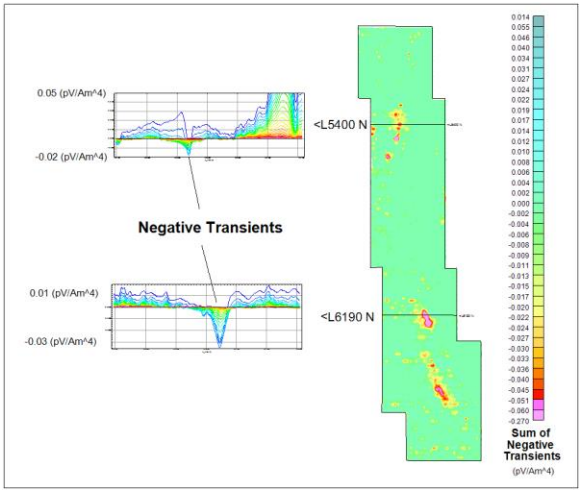

Figure 6: Sum of negative transients and two VTEM profiles, Tullah, Tasmania.

The amplitudes of VTEM data over resistive grounds are relatively now. If the number of decay data in the off-time windows is below a user specified noise threshold, then the decay will be skipped. The calculated AIIP apparent chargeability and resistivity of the study area are shown in Figure . The chargeability map follows the sum of negative transients closely. The sources of the AIIP could be clays or sulphides, or a combination of both.

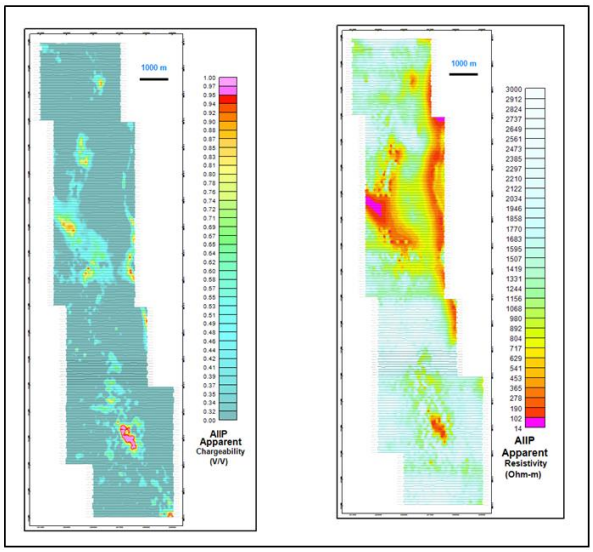

Figure 7: AIIP apparent chargeability and resistivity, Tullah, Tasmania.

DISCUSSION

For real VTEM data contaminated with noise and geology different from uniform half-space, two constraints, a restricted range of inverted apparent resistivity and the use of proper frequency factor, are required in order to for AIIP mapping tool to generate geologically meaningful outputs.

The range of acceptable inverted AIIP apparent resistivity can be estimated by other means and one of them is the Resistivity Depth Imaging (RDI) technique based on the transformation scheme described by Meju (1998).

Extensive discussions on frequency factor are provided in Pelton *et al*. (1978). A reasonable average of frequency factors can be obtained using AIIP forward modeling of VTEM decays of selected locations within a survey area. If the frequency factors are widely distributed, then AIIP mapping should be run using several frequency factors.

CONCLUSION

An improved version of AIIP mapping tool based on Airbeo (CSIRO/AMIRA) has been created for the in-loop VTEM system, which is optimally configured to excite a unique AIIP response, including negative transients in mid to late times over resistive grounds from bodies of modest chargeability. Test results on field VTEM data prove that the new AIIP mapping tool can work, if the inverted resistivity range is restricted and the proper frequency factor is used. The derived AIIP apparent chargeability map provides additional information for the interpretation of VTEM data.

ACKNOWLEDGMENTS

We would like to thank Yunnan Tin Australia Pty Ltd. for permission to use the VTEM data from an area near Tullah, Tasmania for this study. This work is not possible without the source codes from CSIRO/AMIRA project P223F.

REFERENCES

Boyko, W., Paterson, N.R. and Kwan, K., 2001, AeroTEM characteristic and field results: The Leading Edge, **20**, 1130-1138.

Cole, K. and Cole R., 1941, Dispersion and absorption in dielectrics, Part I. Alternating current characteristics: Journal of Chemical Physics, **9**, 341-351.

Corbett, K.D., 2002: Updating the geology of the Mount Read Volcanics belt Western Tasmanian Regional Minerals Program Mount Read Volcanics Compilation: Tasmanian Geological Survey Record 2002/19, Mineral Resources Tasmania, Department of Infrastructure, Energy and Resources, Tasmania.

Han, Lixing and Neumann, Michael, 2006, Effect of dimensionality on the Nelder-Mead simplex method, Optimization Methods and Software, **21**, 1-16.

Kang, S., Oldenburg D.W., Marchant, D., Yang, D. and Haber, E., 2014, On recovering IP information from airborne EM data: presented at Geotech airborne geophysics workshop, AME BC Mineral Exploration Roundup 2014 Conference.

Kratzer, Terence and Macnae, James C., 2012: Induced polarization in airborne EM: Geophysics, **77**, E317-327.

Kwan, K., Prikhodko, A., Legault, Jean M., Plastow, G., Xie, J. and Fisk, K., 2015: Airborne Inductive Induced Polarization Chargeability Mapping of VTEM data, ASEG-PESA 24th International Geophysical Conference and Exhibition, Perth, Australia.

Meju, Maxwell A., 1998: A simple method of transient electromagnetic data analysis: Geophysics, **63**, 405-410.

Nelder, J.A., and Mead, R, 1965: A Simplex Method for Function Minimization, *Computer Journal*, **7(4)**, 308-313.

Oldenburg, Douglas W., Li, Yaoguo and Ellis, Robert G., 1997: Inversion of geophysical data over a copper gold porphyry deposit: a case history for Mt. Milligan: Geophysics, **62**, 1419-1431.

Pelton, W.H., Ward, S.H., Hallof, P.G., Sill, W.R., and Nelson, P.H., 1978, Mineral discrimination and removal of inductive coupling with multi-frequency IP: Geophysics, **43**, 588–609.

Press, W.H., Teukolsky, S.A., Vetterline, W.T. and Flannery, B.P., 2002: Numerical Recipes in C, The Art of Scientific Computing, 2nd Edition, Cambridge University Press.

Raiche, A., 1999, A flow-through Hankel transform technique for rapid, accurate Green's function formulation: Radio Science, **34**, 549-555.

Raiche, A.P., Jupp, D.L.B., Rutter H. and Vozoff, K., 1985, The joint use of coincident loop transient electromagnetic and Schlumberger sounding to resolve layered structures: Geophysics, **50**, 1618-1627.

Seymour, D.B., Green, G.R. and Calver, C.R., 2007: The Geology and Mineral Deposits of Tasmania: A summary: Geological Survey Bulletin, **72**.

Smith, R. S. and J. Klein, 1996, A special circumstance of airborne induced polarization measurements: Geophysics, **61**, 66–73.

Smith, R. S. and West, G.F., 1989, Field examples of negative coincident-loop transient electromagnetic responses modeled with polarizable half-planes: Geophysics, **54**, 1491-1498.

Welhener, H., Labrenz, D., and Huang, J., 2007, Mt. Milligan Project Resource Report, Omenica Mining District: technical report (NI43-101) prepared for Terrane Metals Corp., by Independent Mining Consultants, Inc., 113 p.

Witherly, K., Irvine, R., and Morrison, E.B., 2004, The Geotech VTEM time domain electromagnetic system: SEG, Expanded Abstracts, 1217-1221.

Wright, Margaret, 2012: Nelder, Mead, and the other simplex method, Documenta Mathematica, Extra Volume ISMP, 271-276.

APPENDIX B: Final Deliverables

B1: Databases

A1_ch25t55_aiip_final.gdb;
A2_ch25t55_aiip_final.gdb;
A3_ch20t55_aiip_final.gdb;
A4_ch20t55_aiip_final.gdb;
A5_ch25t55_aiip_final.gdb;

Database channel descriptions;

A1, A2 and A5 blocks

Channel	Descriptions	Unit
x	UTM Easting (NAD83, UTM zone 7N)	meter
y	UTM Northing (NAD83, UTM zone 7N)	meter
radarb	EM TX-RX height above ground	meter
sfzo	Observed dB/dt Z component array (Ch 25 to 55), 31 chs	pV/Am^4
sfzc	Calculated dB/dt Z component array (Ch 25 to 55), 31 chs	pV/Am^4
chg_final	Final AIIP apparent chargeability	V/V
res_final	Final AIIP apparent resistivity	Ohm-m

A3 and A4 blocks

Channel	Descriptions	Unit
x	UTM Easting (NAD83, UTM zone 7N)	meter
y	UTM Northing (NAD83, UTM zone 7N)	meter
radarb	EM TX-RX height above ground	meter
sfzo	Observed dB/dt Z component array (Ch 20 to 55), 36 chs	pV/Am^4
sfzc	Calculated dB/dt Z component array (Ch 20to 55), 36 chs	pV/Am^4
chg_final	Final AIIP apparent chargeability	V/V
res_final	Final AIIP apparent resistivity	Ohm-m

B2: Grids

A#_chg_finalw.grd: AIIP apparent chargeability grids;
A#_res_final.grd: AIIP apparent chargeability grids;